

Measuring ground state properties of fission fragments for the understanding of the r-process

Timo Dickel
GSI Darmstadt, JLU Gießen

Overview

1. Nuclear fission

- History
- Different modes
- Mass yields
- Fission Isomers
- Fission studies at ELI-NP

2. Nucleosynthesis above Iro

- different processes
- s-process
- r-process
- What are the relevant nuclear properties of the isotopes
- The role of fission in the r-process

3. Measuring ground state properties

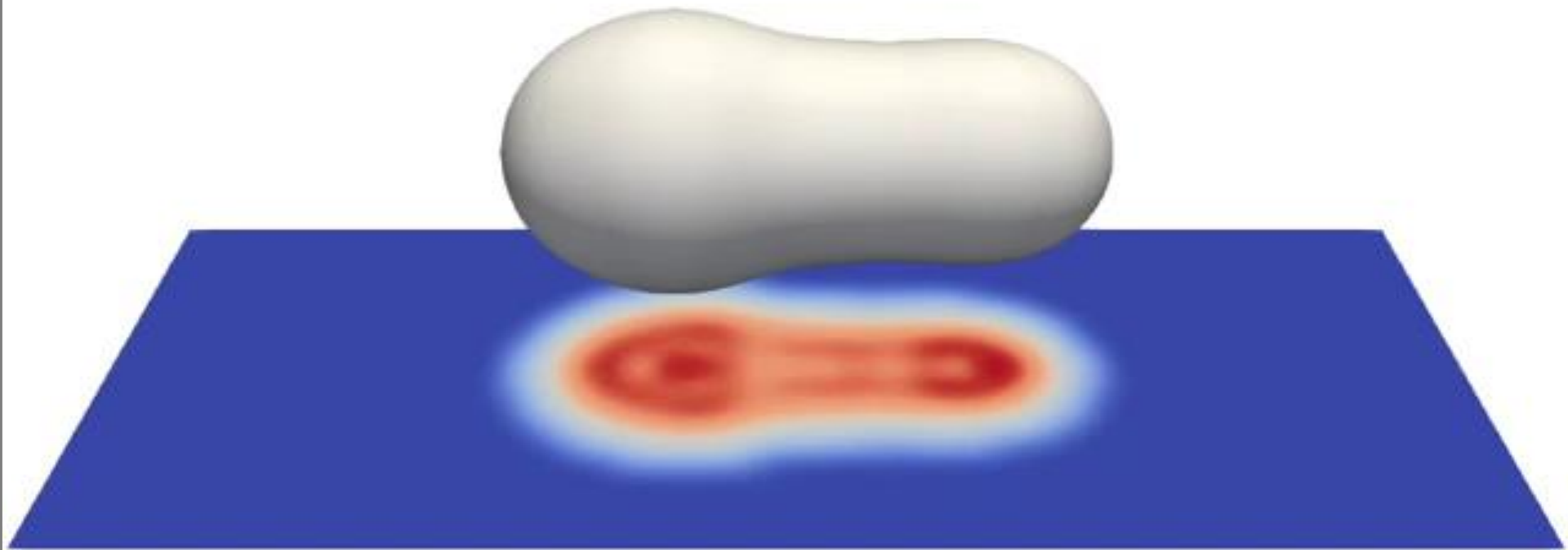
- beta delayed neutron emission
- Half-life
- Mass / Neutron separation energy
- FRS Ion Catcher
- ELISOL

Some historical milestones in fission studies

- 1932 Discovery of the neutron (J. Chadwick)
- 1937 Development of the Liquid Drop Model (N. Bohr)
- 1938 Neutron-induced fission (O. Hahn and F. Strassmann)
Explanation of fission (L. Meitner and O.R. Frisch)
- 1939 Spontaneous fission (^{238}U , G.N. Flerov and K.A. Petrzhak)
- 1942 First self-sustaining chain reaction (E. Fermi)
- 1945 First nuclear bomb (The Manhattan project)
- 1962 Fission isomers (V.M. Polikanov et al.)

Fission – the movie

Time scale for fission from ‘compound nucleus’ to scission ~ 20 zs ($\sim 20 \times 10^{-21}$ s)

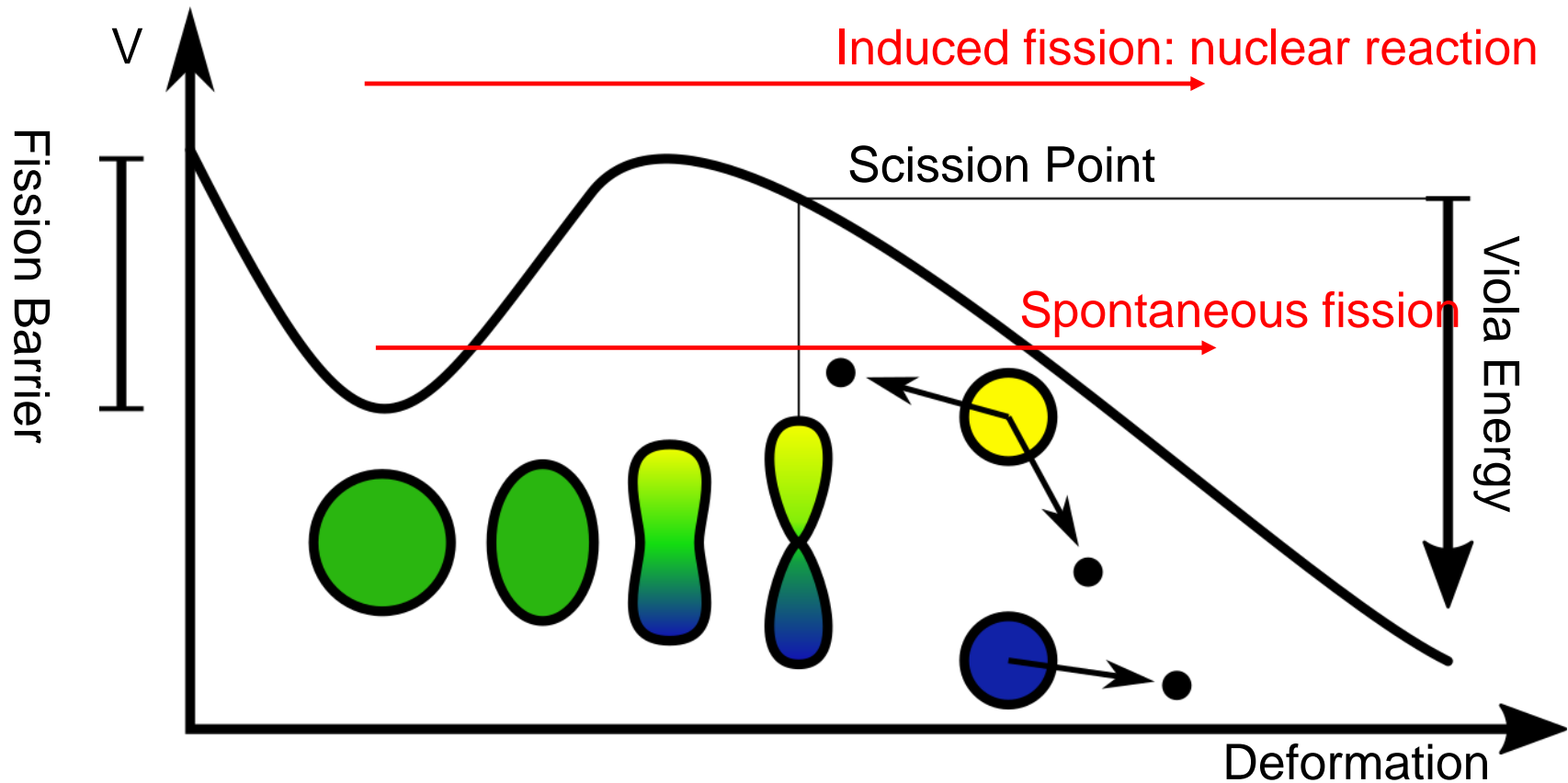


Time-dependent Hartree-Fock + BCS simulations for ^{240}Pu

G. Scamps, C. Seminel, *Nature* **564**, 382–385 (2018)

Schematic view of the fission process

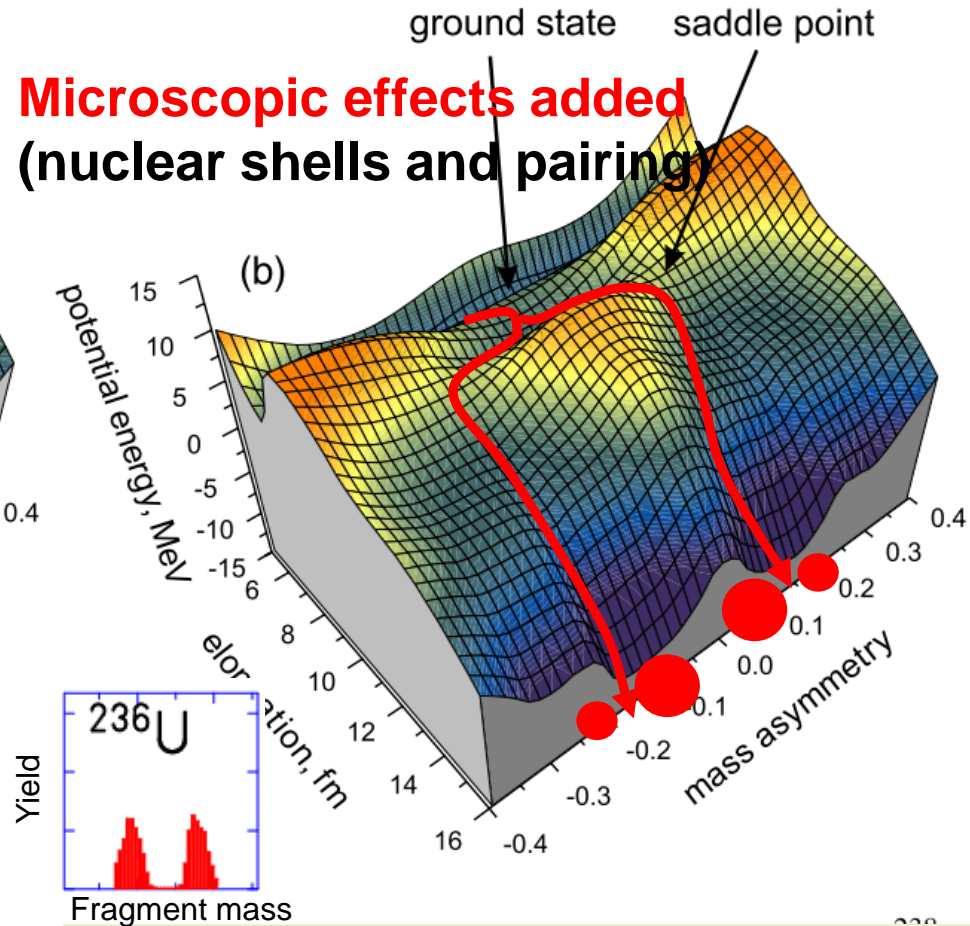
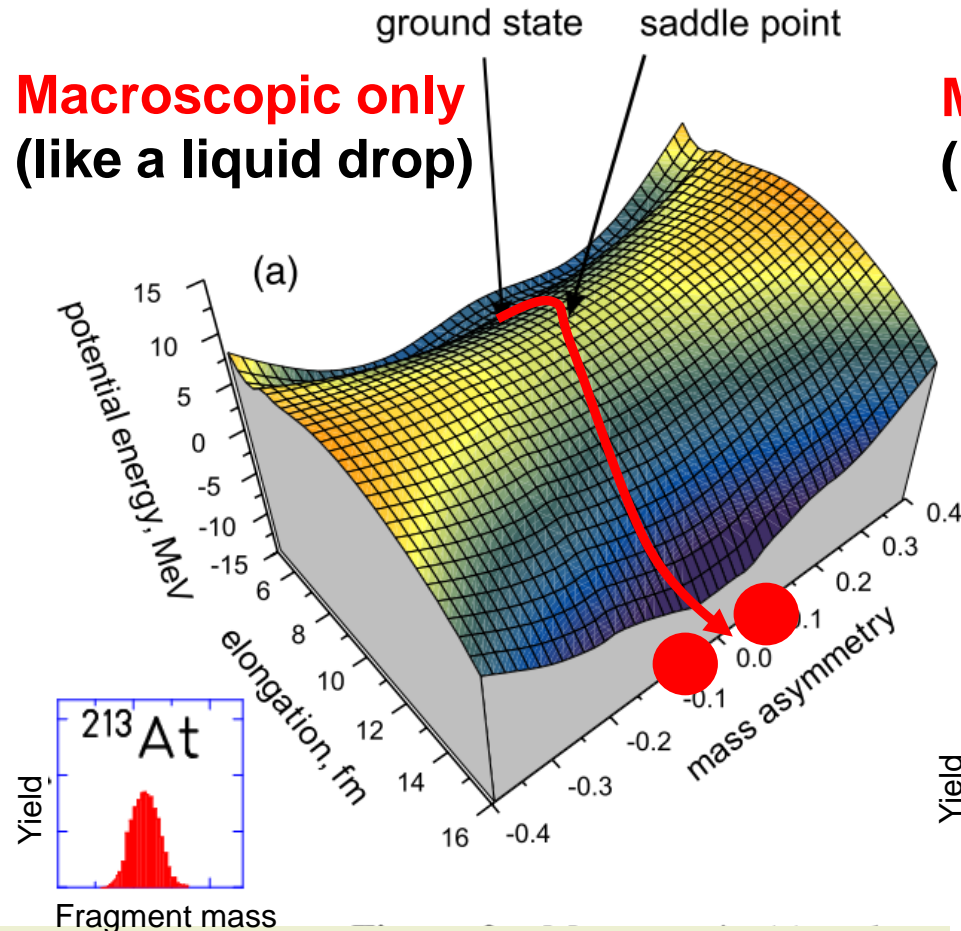
Excitation of the nucleus over fission barrier or tunnel effect



Symmetric vs. asymmetric fission

J. Phys. G: Nucl. Part. Phys. **35** (2008) 035104

A V Karpov *et al*

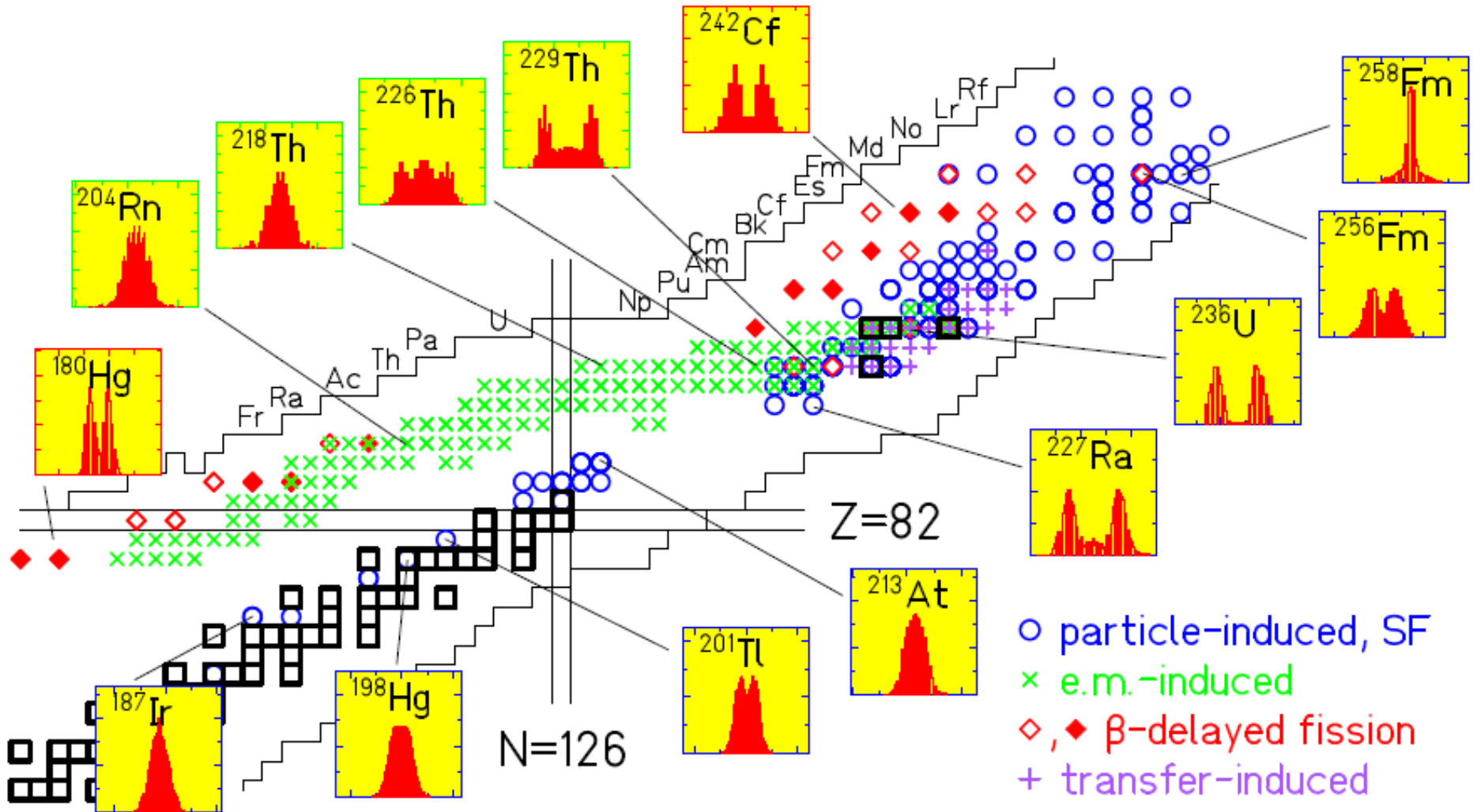


Symmetric Mass Split (single peak)
– when pure LDM (no shell effects)

Asymmetric Mass Split (two peaks)
when shell effects included

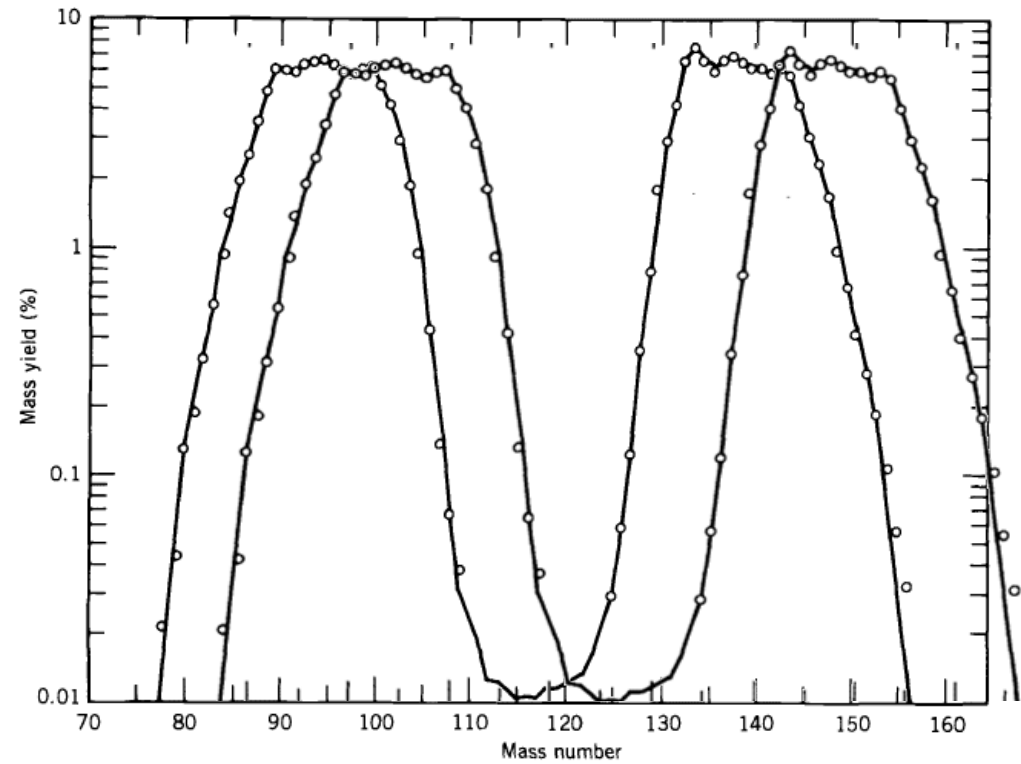
Overview – Activation and FF distributions

Karl-Heinz Schmidt and Beatriz Jurado 2018 Rep. Prog. Phys.81 106301



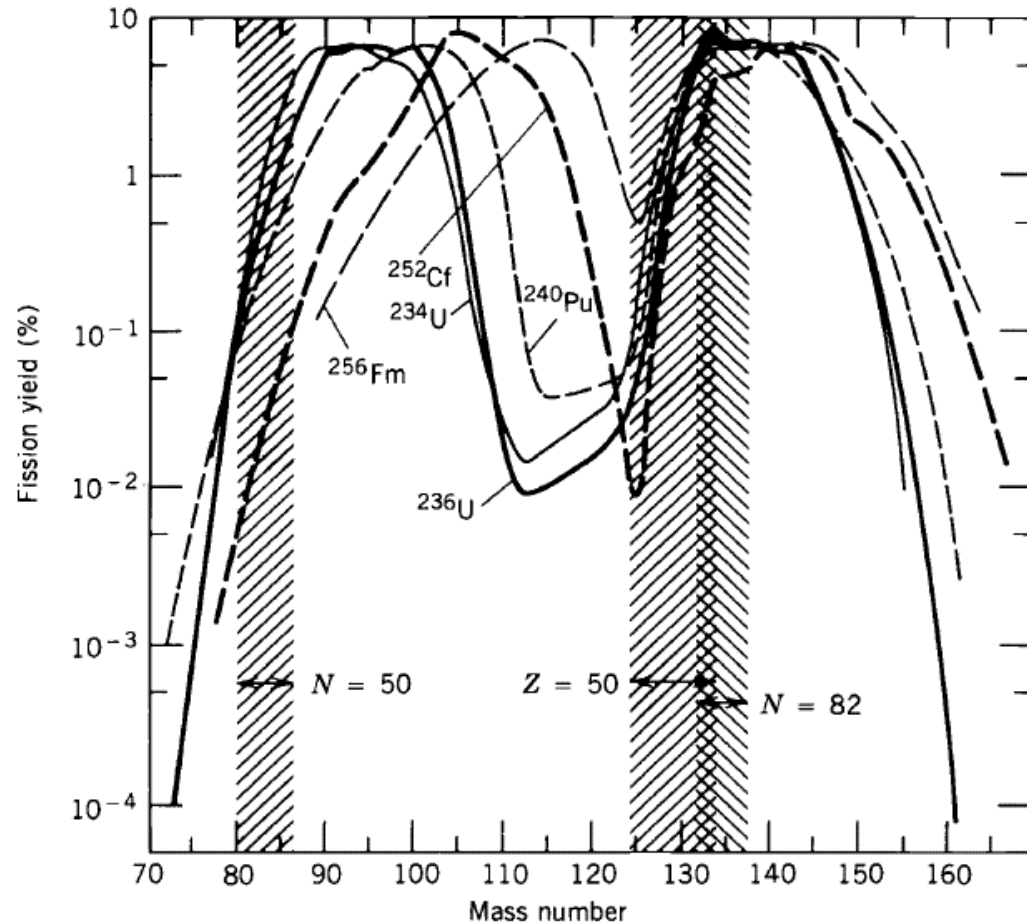
Effect of nuclear shell structure on FF distributions

- When investigating the FF distributions of various actinides, say from ^{236}U to ^{256}Fm , we would expect to have an overall shift of the mass distributions, according to their A ratios

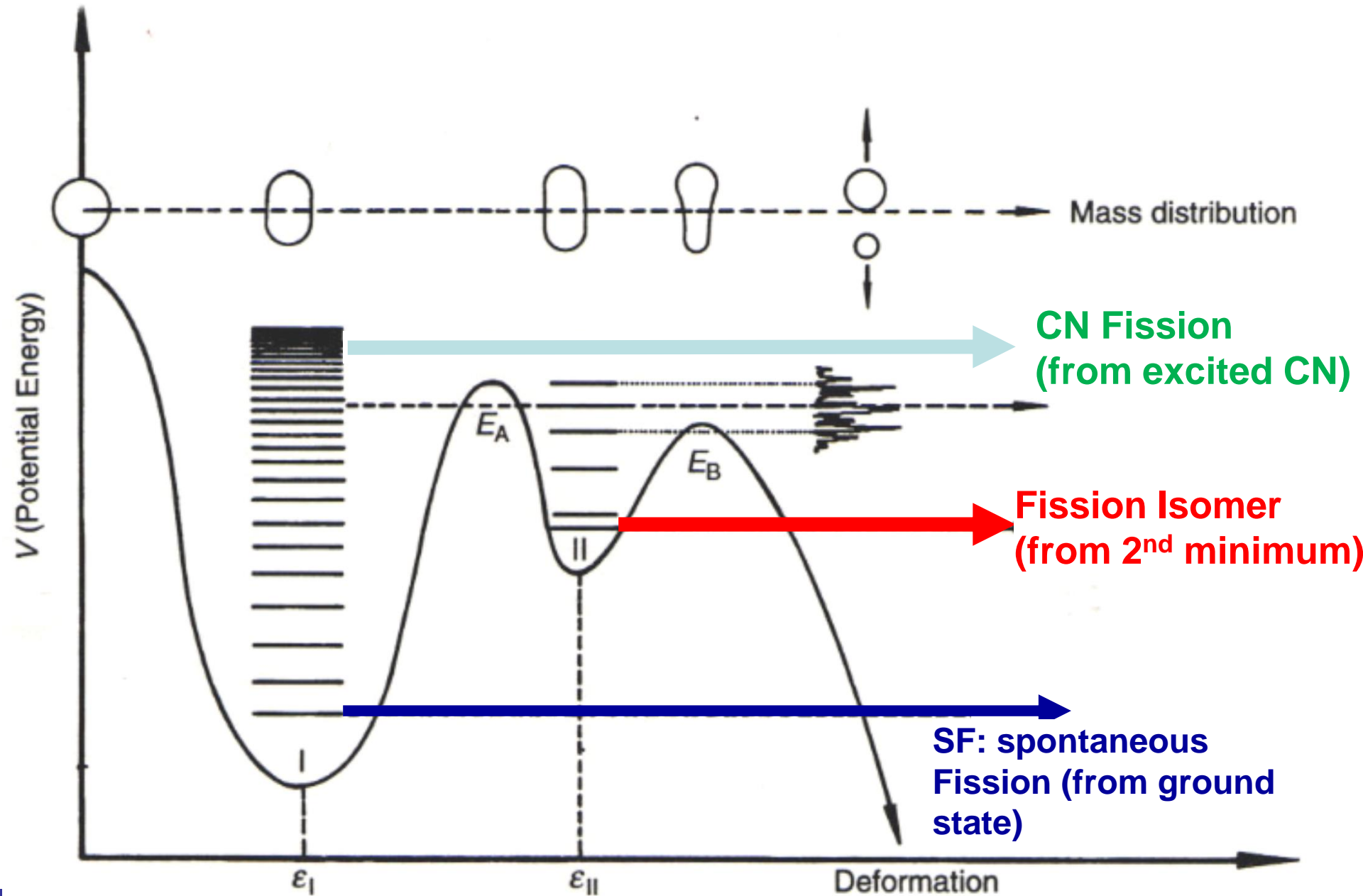


Effect of nuclear shell structure on FF distributions

- However, the experimental data shows a different picture
- The increase in A is **only in the low mass fragments**
- The lowest high-mass fragments are around the **doubly magic** $^{132}_{50}\text{Sn}_{82}$
- The nuclei heavier than ^{236}U 'prefer' that their high-mass fragments 'stay' in the doubly-magic region, to gain **as much energy as possible** in the fission process
- No such doubly-magic nucleus in the low-mass region
- This can be explained **only by the shell model**, and not by the collective LDM model

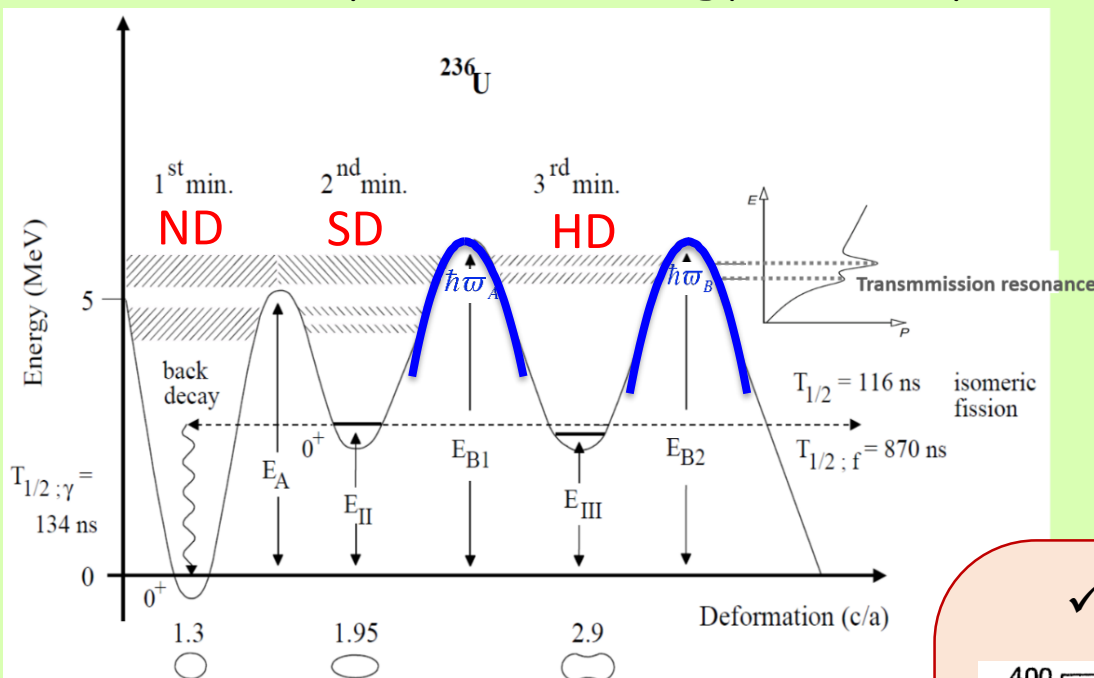


Shape / Fission isomers

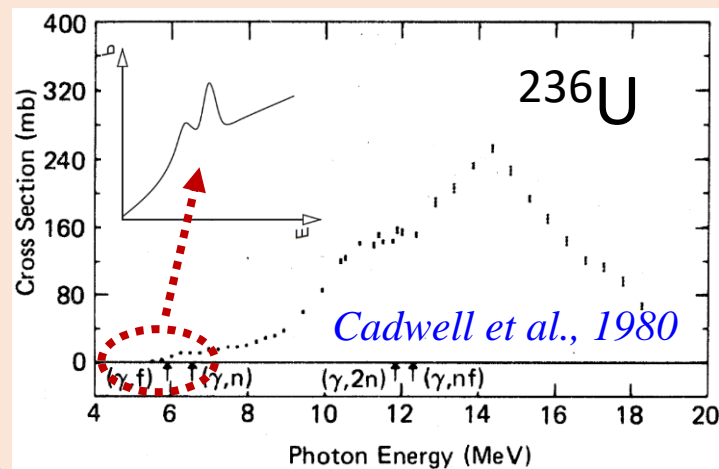


Fission studies with gamma beams at ELI-NP

✓ The potential energy landscape



✓ Fission cross-section

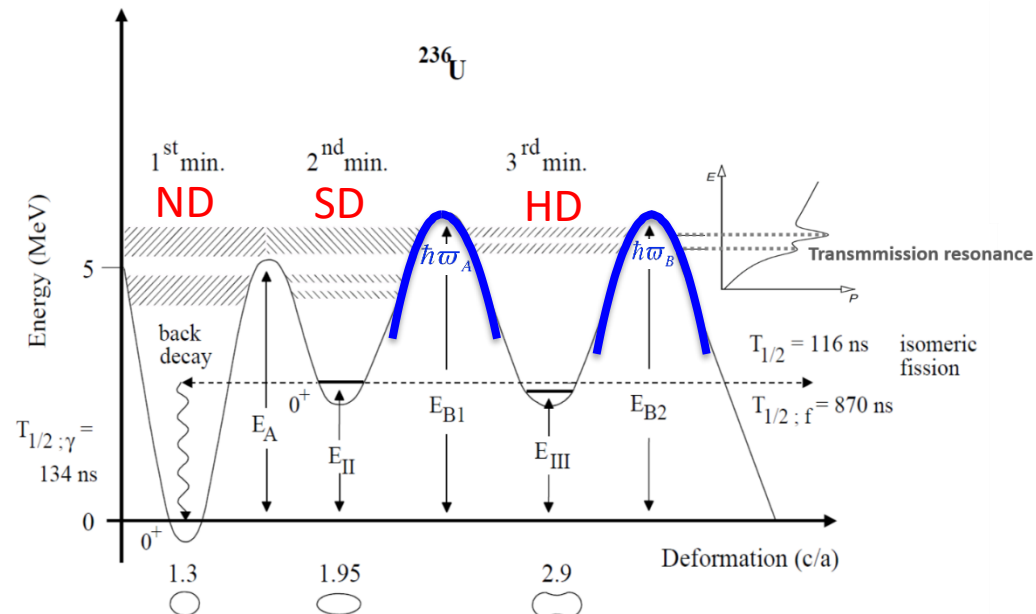


Why photo fission at ELI-NP

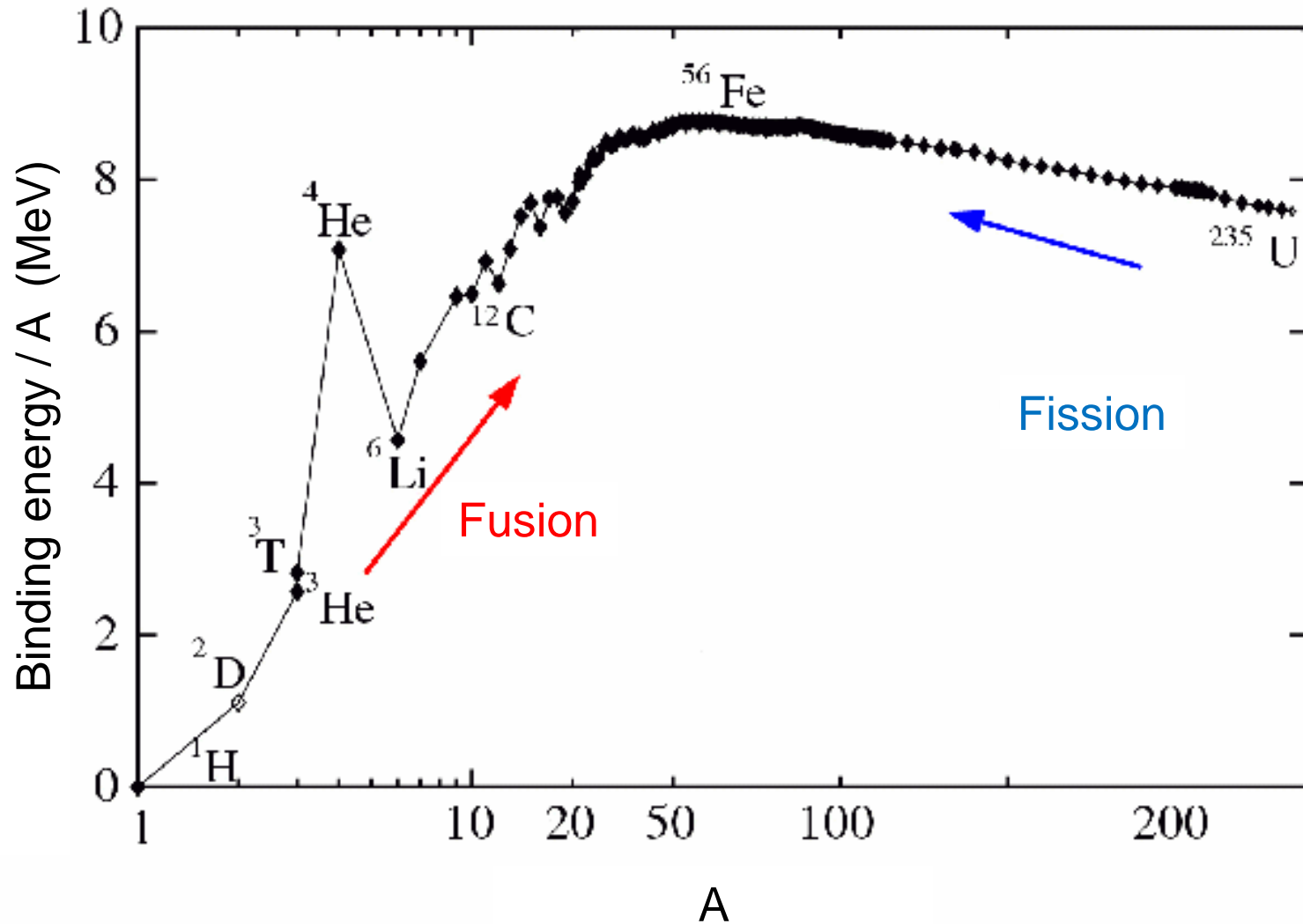
Transfer of well defined amount of angular momentum

Selective investigation of extremely deformed nuclear states

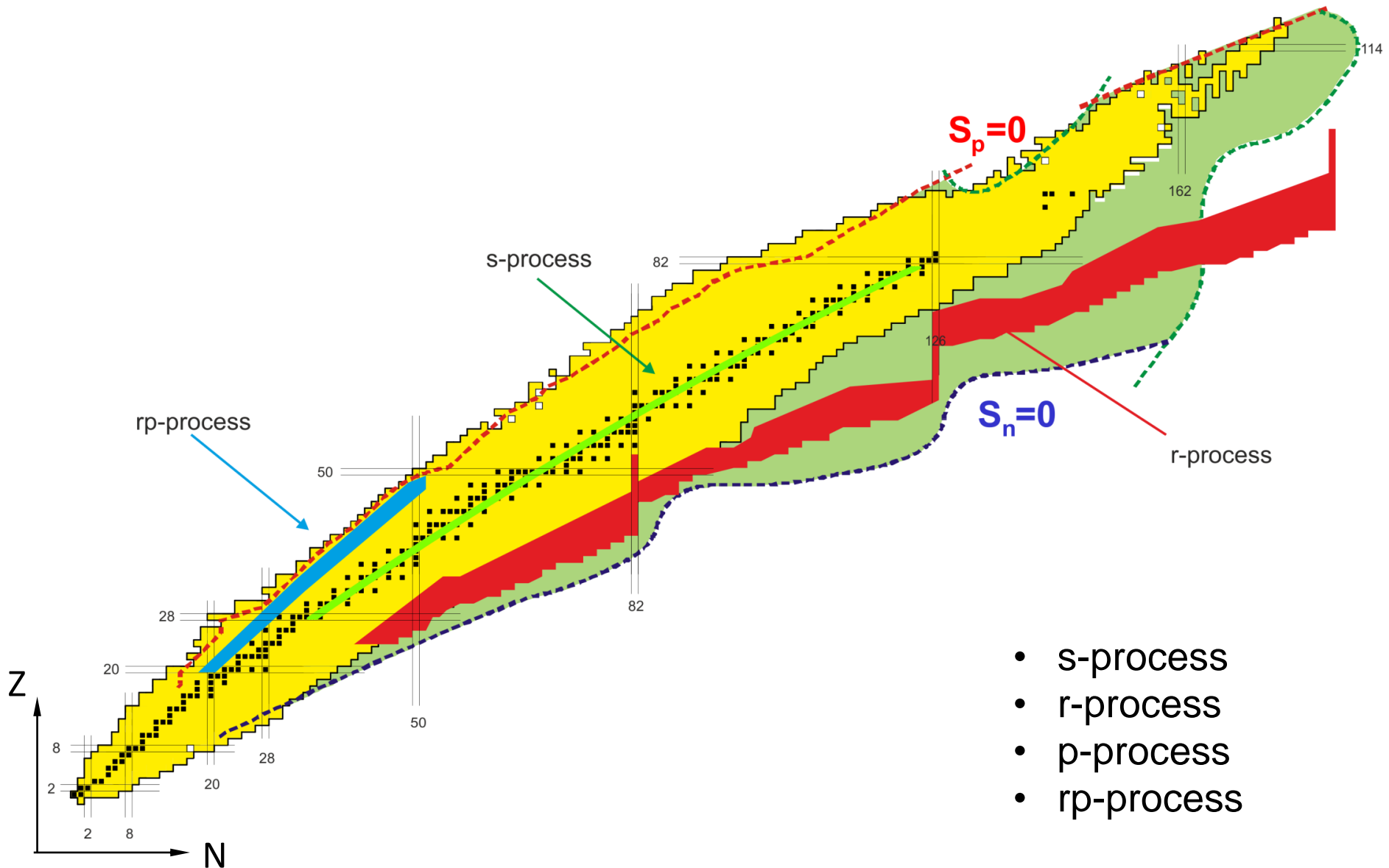
Better understanding of the multiple humped fission barrier landscape



Why fusion goes up to Fe only?

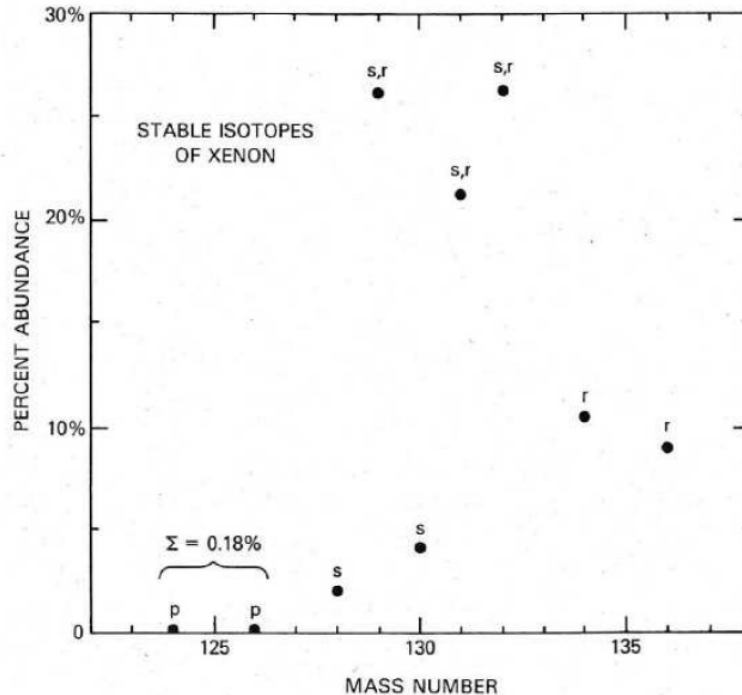


How the elements heavier than Fe are produced?



p, s, r-process: Xe isotopes

Ba 125 8.0 m 3.5 m	Ba 126 100 m	Ba 127 1.9 s 12.7 m	Ba 128 2.43 d	Ba 129 2.13 h 2.20 h	Ba 130 0.106	Ba 131 14.5 m 11.5 d	Ba 132 0.101	Ba 133 36.9 h 10.5 a	Ba 134 2.417	Ba 135 26.7 h 6.592	Ba 136 7.854	Ba 137 2.55 m 11.23	Ba 138 71.70	Ba 139 83.06 m
Cs 124 6.3 s 30.8 s	Cs 125 45 m	Cs 126 1.6 m	Cs 127 6.25 h	Cs 128 3.8 m	Cs 129 32.06 h	Cs 130 3.46 m 29.21 m	Cs 131 9.69 d	Cs 132 6.47 d	Cs 133 100	Cs 134 2.90 h 2.06 a	Cs 135 53 m 2 · 10 ⁶ a	Cs 136 19 s 13.16 d	Cs 137 30,17 a	Cs 138 2.90 m 32.2 m
Xe 123 2.08 h	Xe 124 0.10	Xe 125 57 s 16.9 h	Xe 126 0.09	Xe 127 70 s 36.4 d	Xe 128 1.91	Xe 129 8.89 d 26.4	Xe 130 4.1	Xe 131 11.9 d 21.2	Xe 132 26.9	Xe 133 2.19 d 5.25 d	Xe 134 10.4	Xe 135 15.3 m 9.10 h	Xe 136 8.9	Xe 137 3.83 m
I 122 3.6 m	I 123 13.2 h	I 124 4.15 d	I 125 59.41 d	I 126 13.11 d	I 127 100	I 128 25.0 m	I 129 1.57 · 10 ⁷ a	I 130 9.0 m 12.36 h	I 131 8.02 d	I 132 83.6 m 2.30 h	I 133 9 s 20.8 h	I 134 3.5 m 52.0 m	I 135 6.61 h	I 136 45 s 84 s
Te 121 154 d 16.8 d	Te 122 2.603	Te 123 0.908	Te 124 4.816	Te 125 57.4 d 7.139	Te 126 18.95	Te 127 109 d 9.35 h	Te 128 31.69	Te 129 33.6 d 69.6 m	Te 130 33.80	Te 131 30 h 25.0 m	Te 132 76.3 h	Te 133 55.4 m 12.5 m	Te 134 41.8 m	Te 135 18.6 s



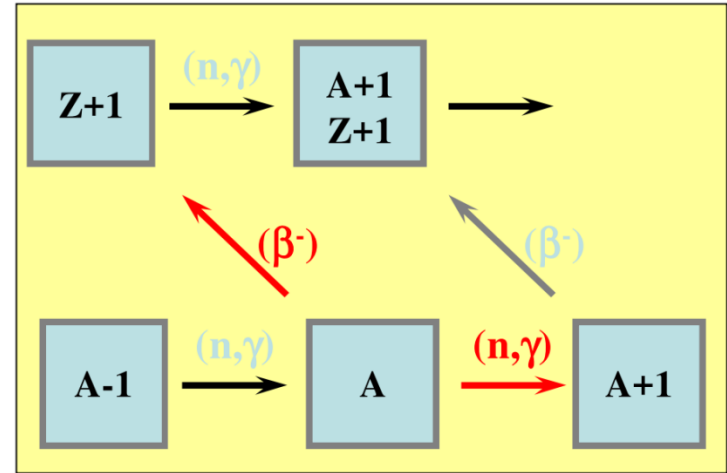
- isotope shielding
- isotopes can be produced in one or several processes
- p-process is more rare

s-process

Where? Under what conditions?

- red giants
- temperature ~ 30 keV ($T_8 \sim 3$)
- neutron densities $\sim 10^{6...8}$ cm $^{-3}$

Where do neutrons come from? $T_{1/2}(n) = 612$ s
 \rightarrow have to be produced somehow!



- $^{13}\text{C}(\alpha, n)^{16}\text{O} + 2.20$ MeV
- $^{17}\text{O}(\alpha, n)^{20}\text{Ne} + 0.60$ MeV
- $^{18}\text{O}(\alpha, n)^{21}\text{Ne} - 0.70$ MeV
- $^{21}\text{Ne}(\alpha, n)^{24}\text{Mg} + 2.58$ MeV
- $^{22}\text{Ne}(\alpha, n)^{25}\text{Mg} - 0.48$ MeV
- $^{25}\text{Mg}(\alpha, n)^{28}\text{Si} + 2.67$ MeV

abundant mother nuclide
fast reaction rate

- $^{13}\text{C}(\alpha, n)^{16}\text{O} + 2.20$ MeV
- $^{22}\text{Ne}(\alpha, n)^{25}\text{Mg} - 0.48$ MeV

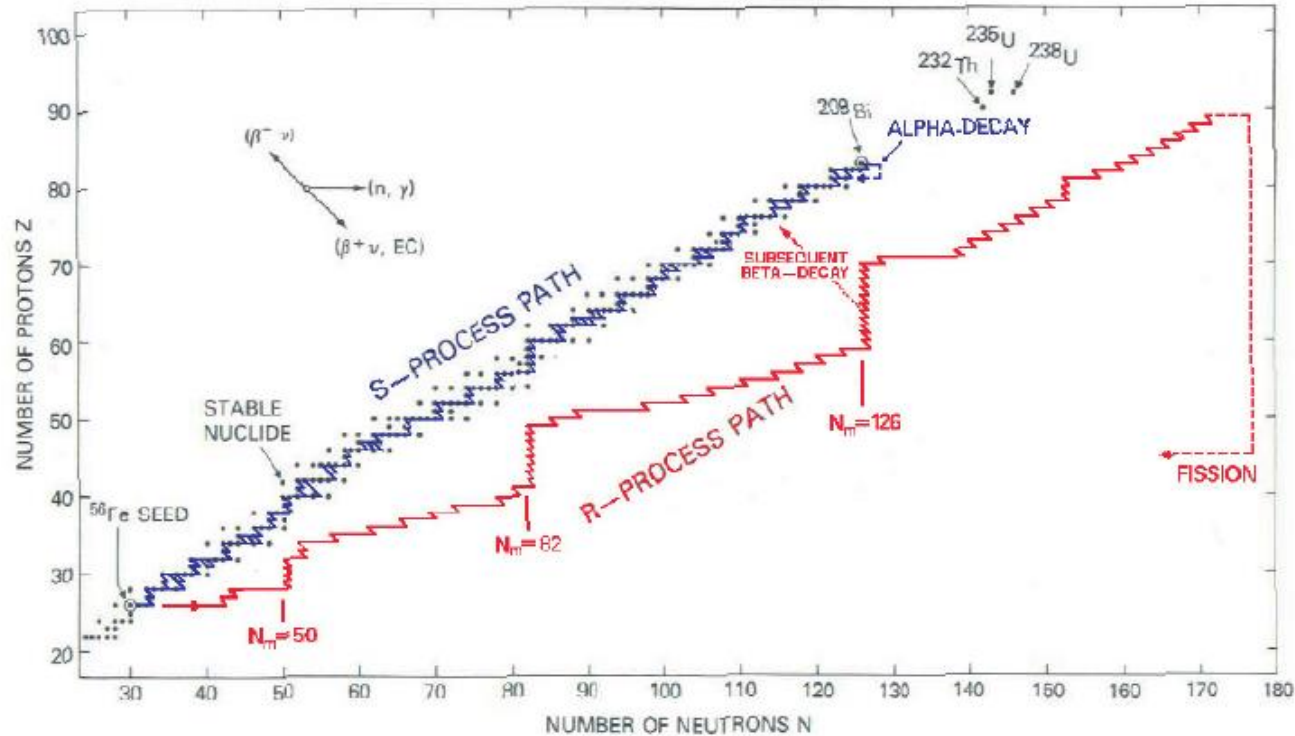
Eu 148 55,6 d $\epsilon; \beta^+ \dots$ α 2,63 γ 550; 630; 611...	Eu 149 93,1 d ϵ γ 328; 277...	Eu 150 12,8 h 36,9 a β^- 1,0 ϵ β^+ ... γ 334; 439; 407... 584...	Eu 151 47,8 σ 4 + 3150 + 6000	Eu 152 96 m 9,3 h 13,33 a β^- 1,9 $\epsilon; \beta^+ \dots$ γ 841; 1,5; 963... 344...
Sm 147 15,0 $1,06 \cdot 10^{11}$ a α 2,235 σ 56	Sm 148 11,3 $7 \cdot 10^{15}$ a α 1,96 σ 2,4	Sm 149 13,8 σ 40100	Sm 150 7,4 σ 102	Sm 151 93 a β^- 0,1... γ (22...); e^- σ 15200
Pm 146 5,53 a $\epsilon; \beta^-$ 0,8... γ 454; 747; 736... σ 8400	Pm 147 2,62 a β^- 0,2... γ (121...) σ 94 + 96	Pm 148 41, d 5,37 d β^- 1,1 γ 550; 1465; γ (76...); e^- σ 10600 $\sigma \sim 1000$	Pm 149 53,1 h β^- 1,1... γ 286... σ 1400	Pm 150 2,7 h β^- 2,3; 3,4... γ 334; 1325; 1166...
Nd 145 8,30 σ 47	Nd 146 17,19 σ 1,4	Nd 147 10,98 d γ 91; 531... σ 400	Nd 148 5,76 σ 2,5	Nd 149 1,73 h β^- 1,4; 1,6... γ 211; 114; 270...
Pr 144 7,2 m 17,3 m γ 59 β^- ... γ (697; 814...)	Pr 145 5,98 h β^- 1,8... γ (748; 676...)	Pr 146 24,0 m β^- 4,1... γ 454; 1525...	Pr 147 13,6 m β^- 2,1; 2,7... γ 315; 641; 578; 78...	Pr 148 2,0 m 2,27 m β^- ... γ 302; 451; 698...

r-process

Mechanism is similar to s-process: n-capture / β^- - decay

BUT : $\lambda_\beta \ll \lambda_n$, neutron densities of $> 10^{22} \text{ cm}^{-3}$

Path lies far away from stability and ends with fission of heavy elements



Nuclear physics input

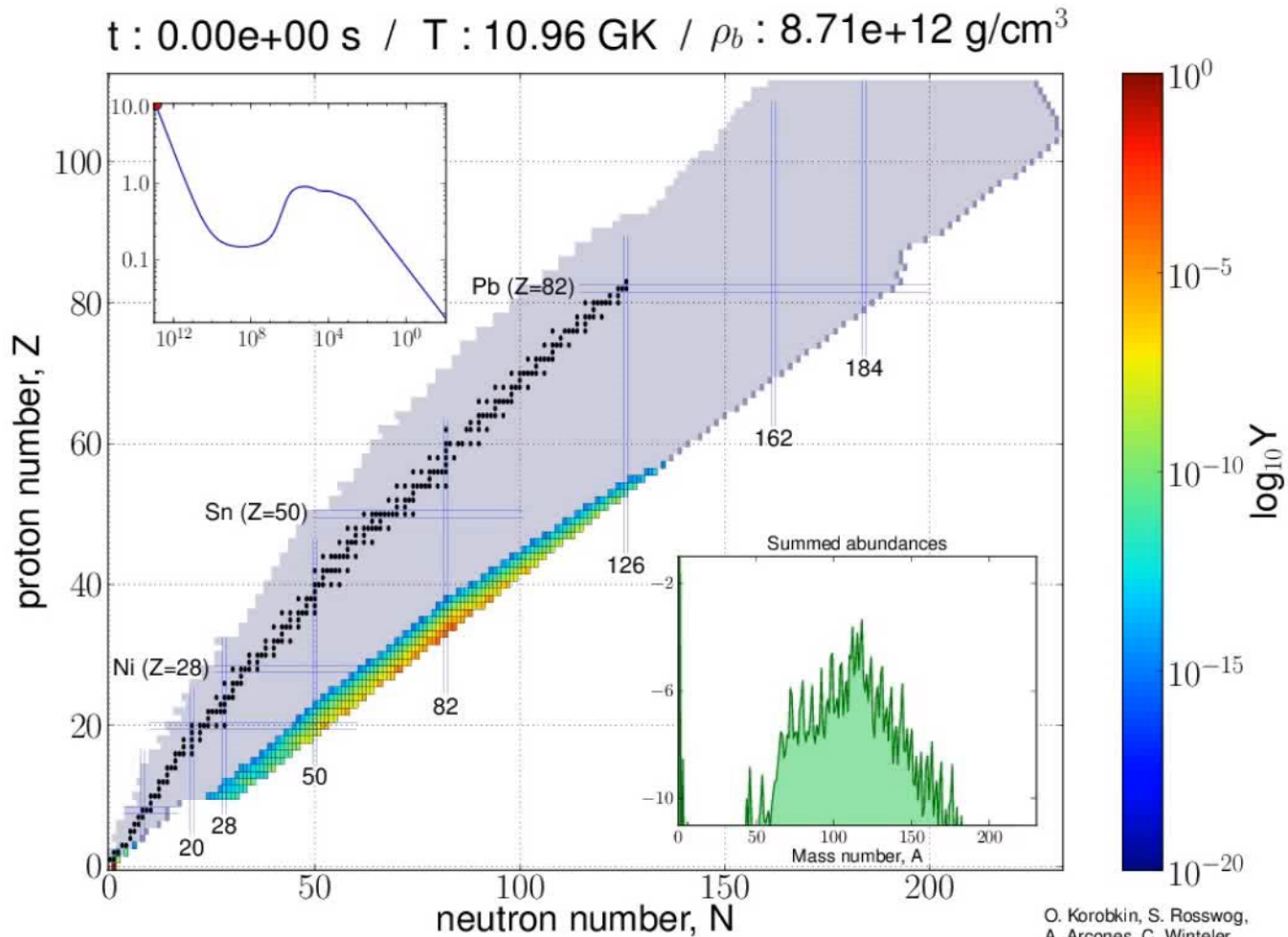
- Masses $\rightarrow S_{2N}$
- Neutron capture cross-sections
- γ induced dissociation cross-sections
- β^- decay half-lives
- Neutron emission, β^- -delayed neutron emission
- Fission, fission fragment distributions, β^- -delayed fission
- α -decay, β^- -delayed α decay

Path

Abundances

Light curve

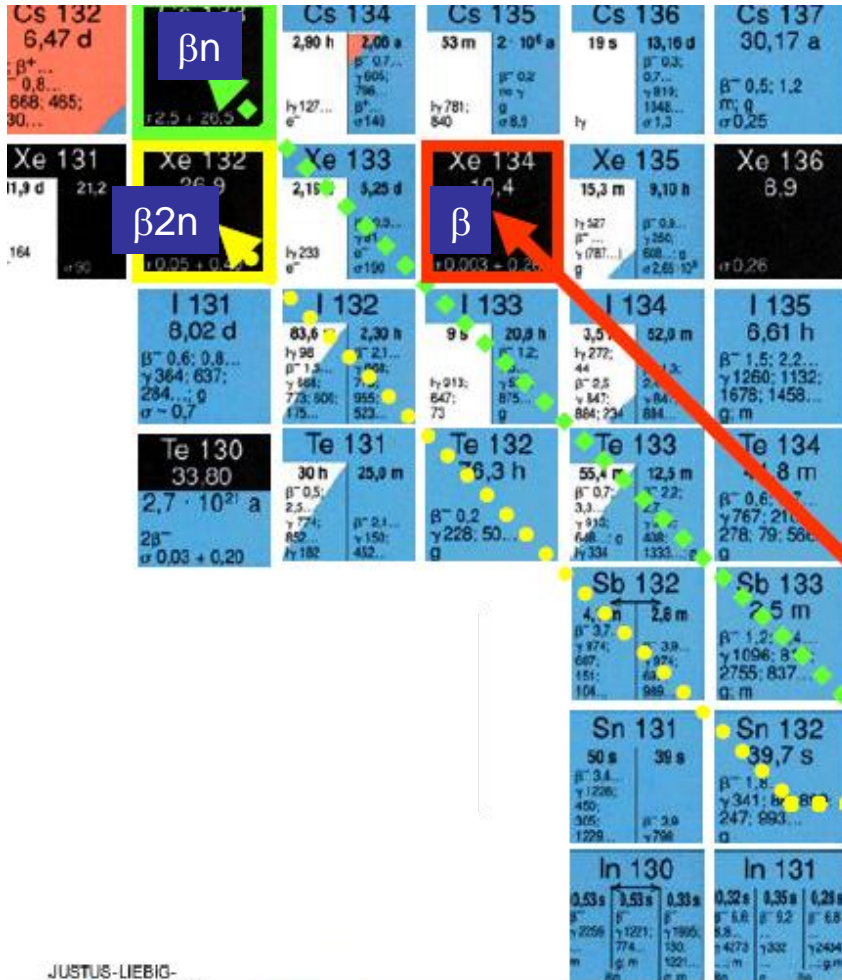
R-process demonstration



O. Korobkin, S. Rosswog,
A. Arcones, C. Winteler,
arXiv:1206.2379

<http://compact-merger.astro.su.se/movies.html#rproc>

Importance of β -delayed neutron emission



During „Freeze-out“:
 detour of β -decay chains
 \Rightarrow *r-abundance changes*

In this case, P_{1n} and P_{2n}
 values of ^{134}In affect the
 relative abundances of ^{134}Xe ,
 ^{133}Cs , ^{132}Xe .

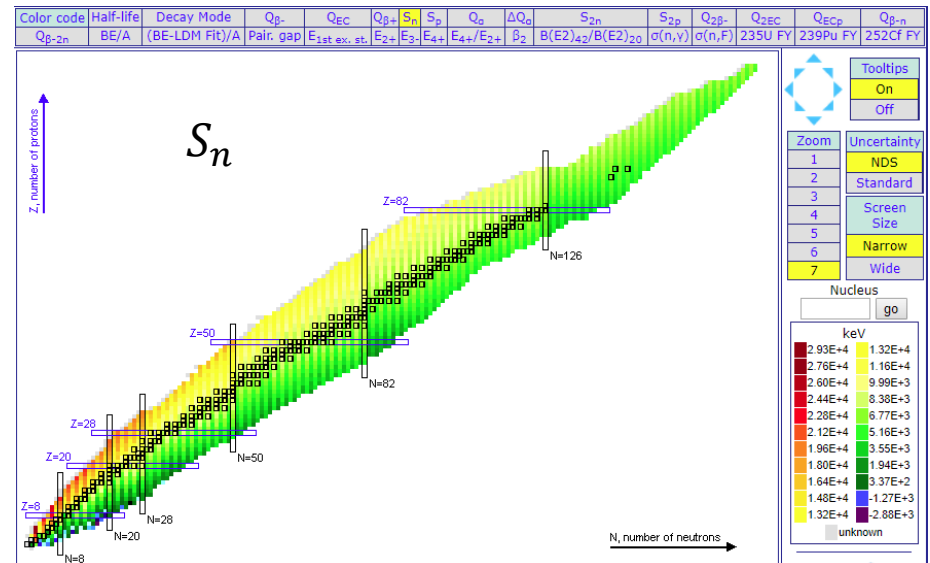
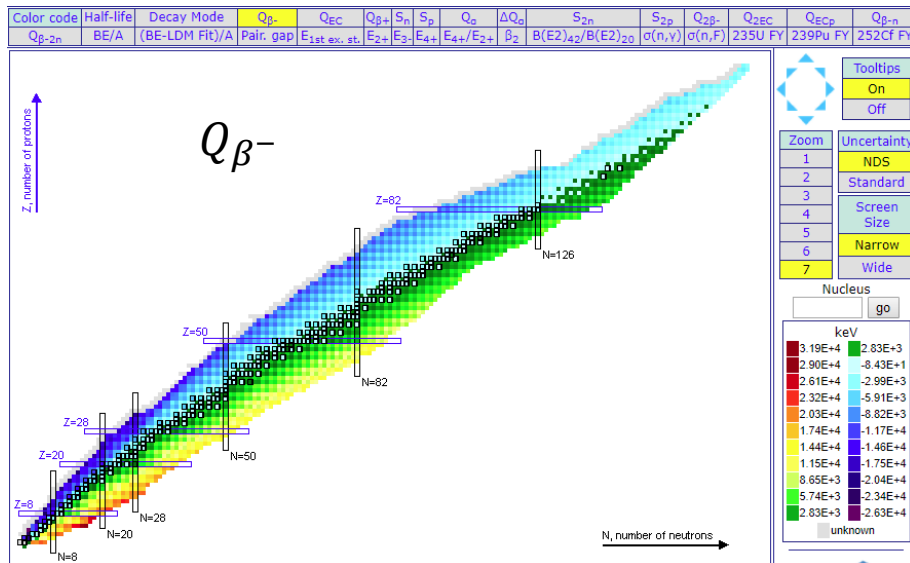
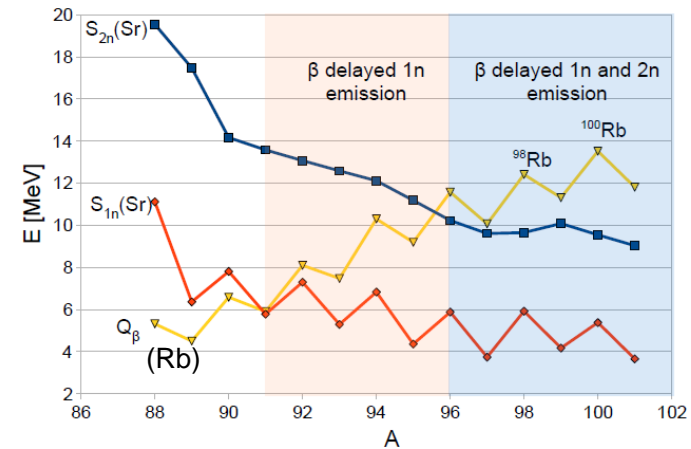
Also, β -delayed neutrons
 introduce more neutrons that
 can be captured.

Beta-delayed neutron emission

- The energetic condition for β -delayed x -nucleon emission is:

$$Q_{\beta^-} \left(\begin{smallmatrix} A \\ Z \\ X \end{smallmatrix} N \right) > S_{x(p)} \left(\begin{smallmatrix} A \\ Z+1 \\ X' \end{smallmatrix} N-1 \right)$$

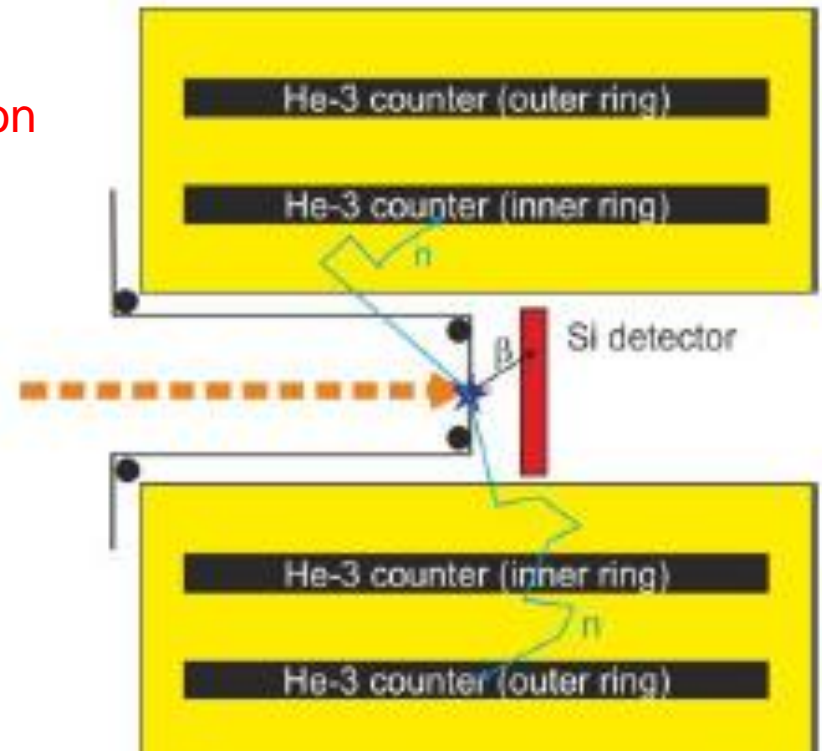
- Since Q_{β^-} increases and S_{xn} decreases as we move away from stability, the probability increases in these regions



The “standard” P_{xn} measurement methods

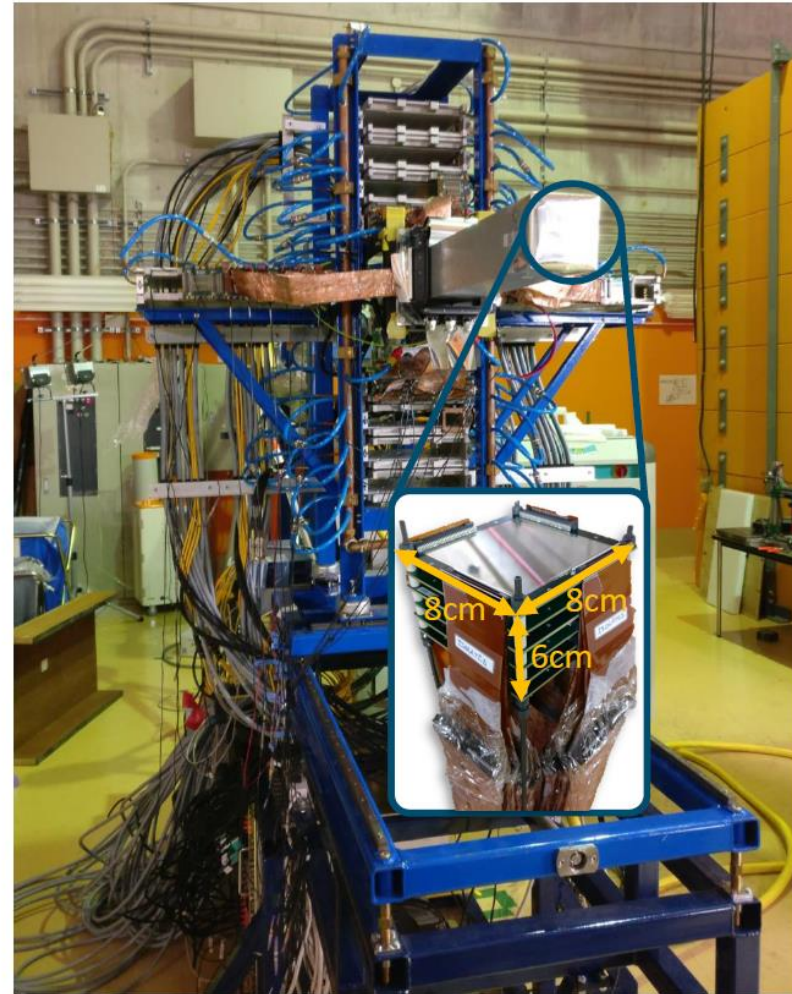
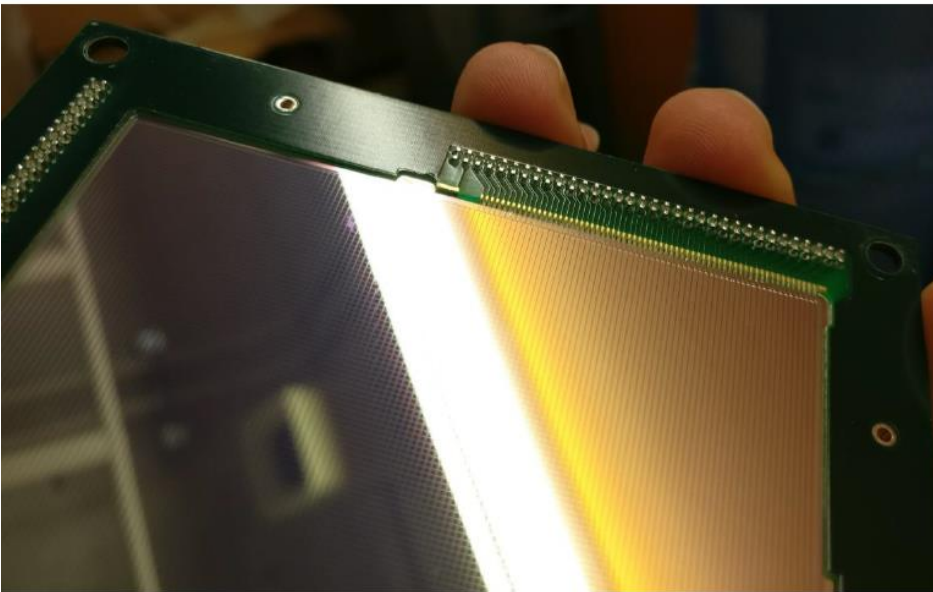
β +xn coincidence

- In addition to P_{xn}, can yield neutron angular correlations
- In addition to P_{xn}, half-lives are measured
- Detection of neutron is challenging
 - Efficiency for detecting β xn decreases with x
 - Detectors energy dependent efficiency requires a-priori knowledge of β & n spectra
 - Prone to single and multiple neutron background



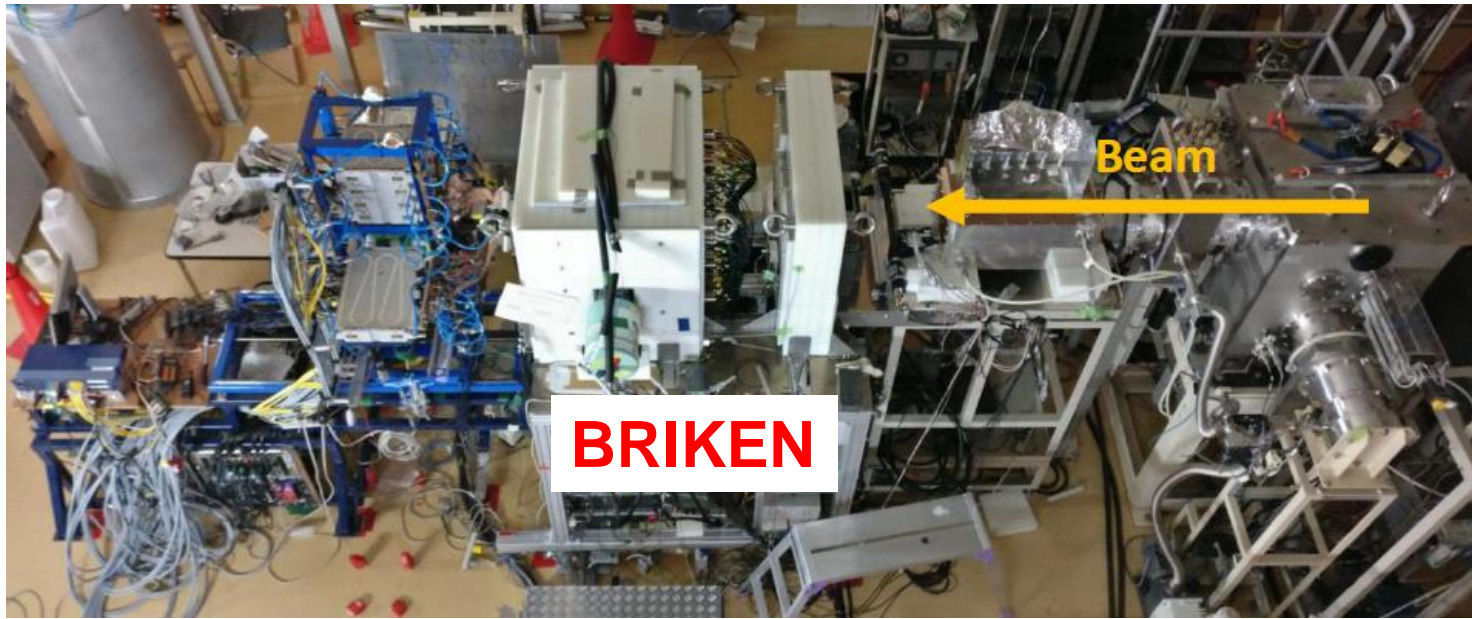
AIDA

- Advanced Implantation Detector Array
- Edinburgh led project
- Built around Double-sided Silicon Strip Detectors (DSSD)

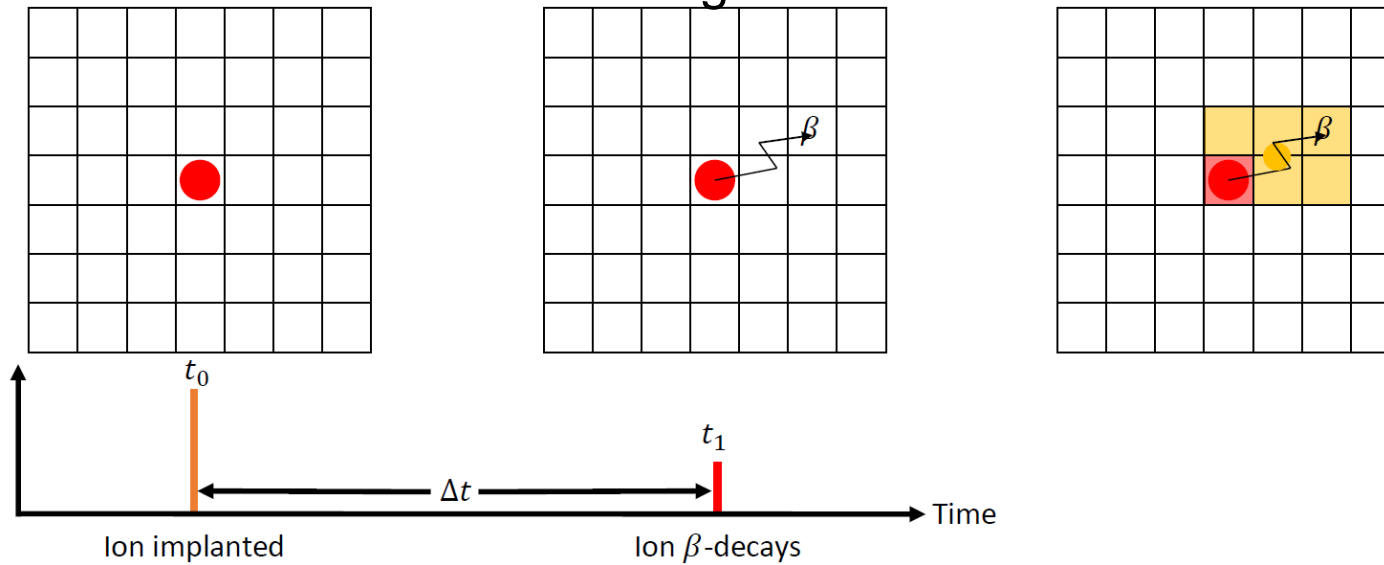


Most beta half-life in the last decade or two have been measured with DSSDs

DSSDs / AIDA

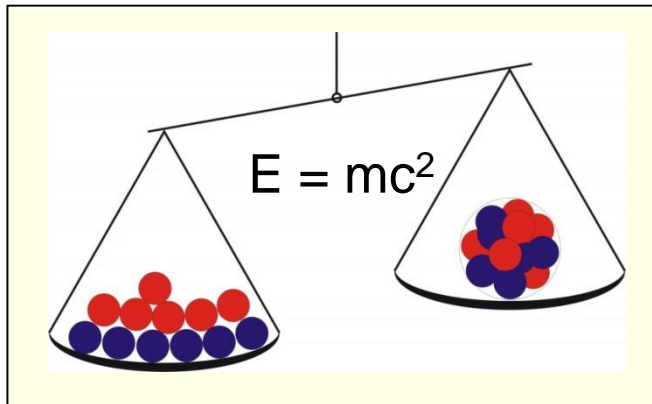


Measuring half-lives



Mass and Binding Energy

The mass of an atomic nucleus reflects its binding energy and hence its stability and structure



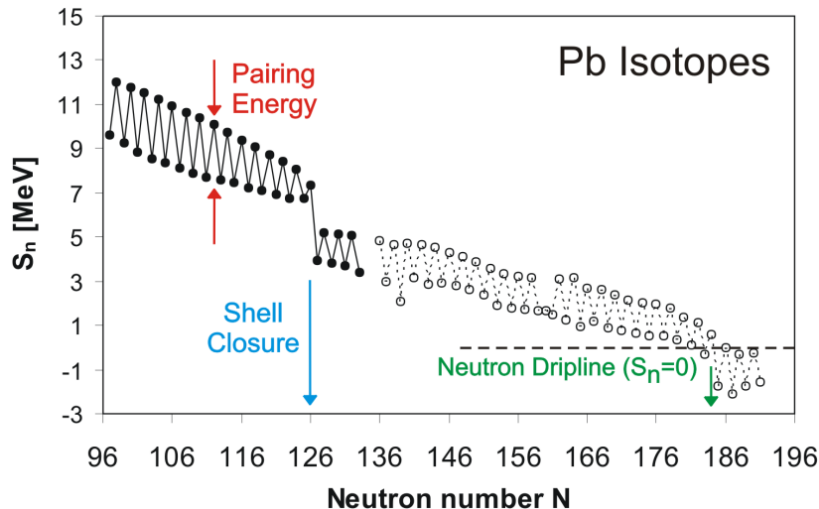
Z Protons (Proton number)

N Neutrons (Neutron number)

A = N + Z (Mass number)

B = Binding energy

Nuclear mass: $M(N, Z) = Z \cdot m_p + N \cdot m_n - B(N, Z)/c^2$



$$S_n = m({}^{A-1}_Z X_{N-1}) + m(n) - m({}^A_Z X_N)$$

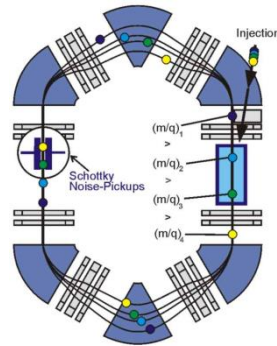
Structure & Dynamics
of Exotic Nuclei

Mass measurement techniques for exotic nuclei

Storage Rings

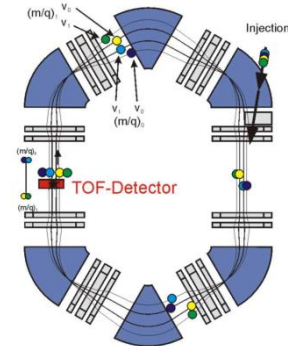
Schottky MS

$t_{\text{meas}} \sim 10 \text{ s}$
 $m/\Delta m = 10^6$
 $\delta m/m \sim 2 \cdot 10^{-7}$
 broadband



Isochronous MS

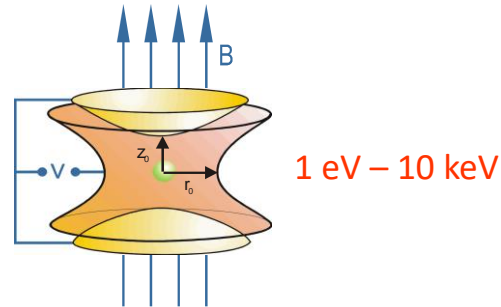
$t_{\text{meas}} \sim 100 \mu\text{s}$
 $m/\Delta m = 2 \cdot 10^5$
 $\delta m/m \sim 10^{-6}$
 broadband



$\sim 500 \text{ MeV/u}$

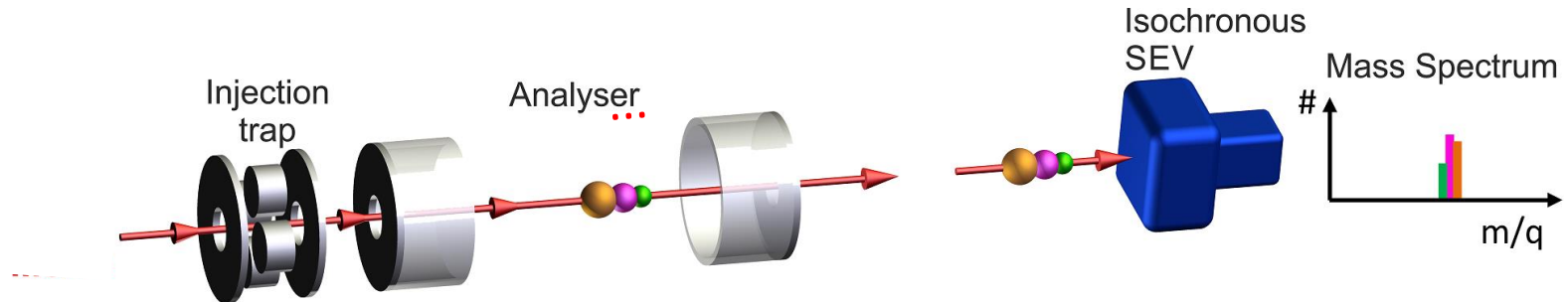
Penning Trap MS (TOF-ICR-MS)

$t_{\text{meas}} \sim 1 \text{ s}$
 $m/\Delta m = 10^6 - 10^7$
 $\delta m/m < 10^{-7}$
 scanning



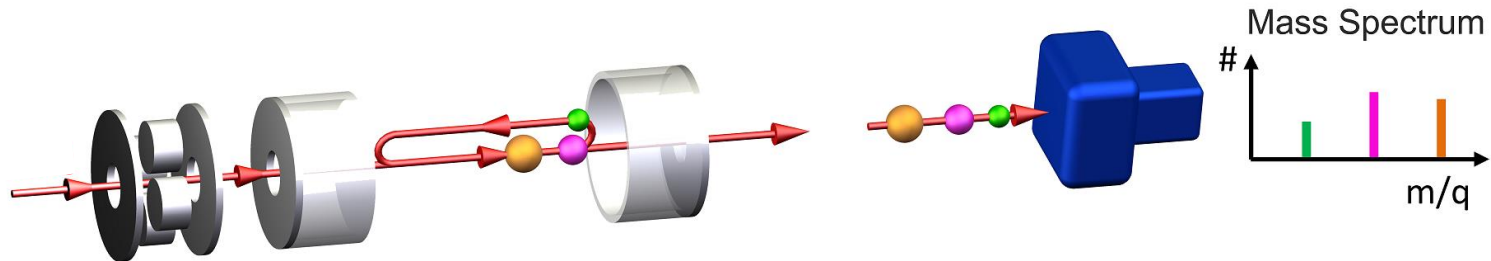
TOF Mass Spectrometry for diagnosis and separation

- Fast → access to very short-lived ions ($T_{1/2} \sim \text{ms}$)
- Sensitive, broadband, non-scanning → efficient, access to rare ions



To achieve high mass resolving power and accuracy:

Multiple-reflection time-of-flight mass spectrometer (MR-TOF-MS)



H. Wollnik et al., *Int. J. Mass Spectrom. Ion Processes* 96 (1990) 267

Applications

- Diagnostics measurements: monitor production, separation and low-energy beam preparation of exotic nuclei
- Direct mass measurements of exotic nuclei
- High-resolution mass separator

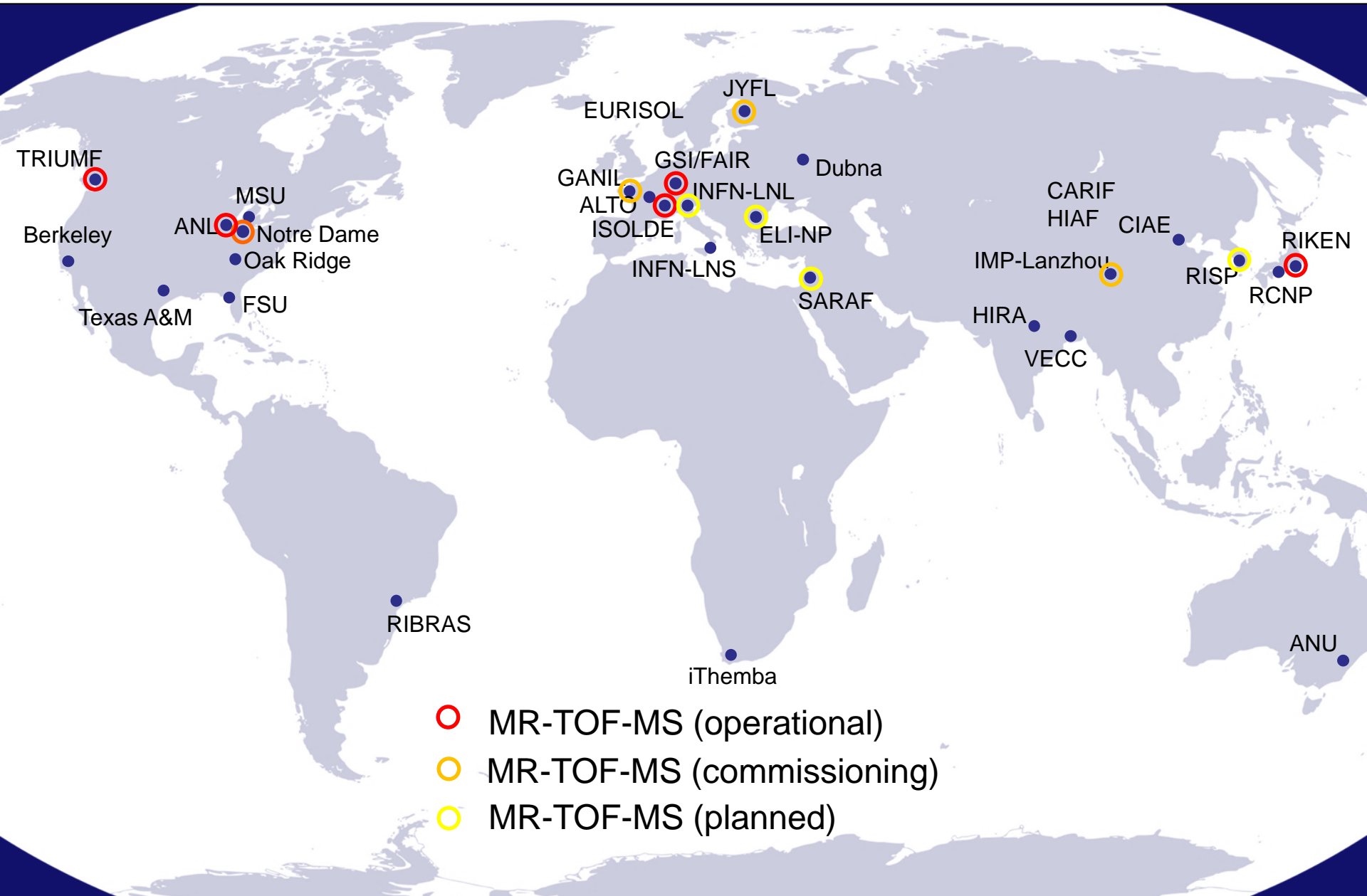
W.R. Plaß et al., *Int. J. Mass Spectrom.* 394 (2013) 134

C. Scheidenberger et al., *Hyperfine Interact.* 132 (2001) 531

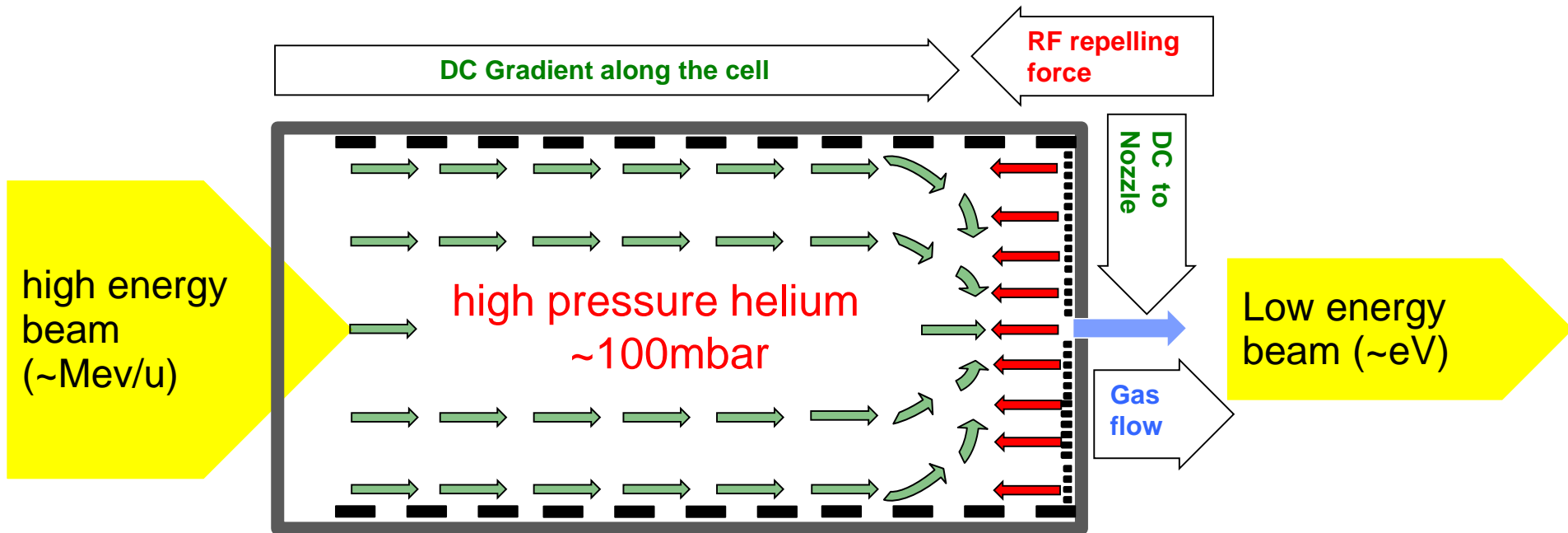
W.R. Plaß et al., *NIM B* 266 (2008) 4560

T. Dickel et al., *Phys. Lett. B* 744 (2015) 137

MR-TOF-MS in RIB Facilities



Thermalizing fast reaction products for precision studies



IGISOL/Stopping cells:

- **Fast** \rightarrow access to short-lived exotic nuclides ($T_{1/2} \sim$ ms)
- **Universal** \rightarrow element-independent
- **Efficient** \rightarrow highest stopping and extraction efficiency

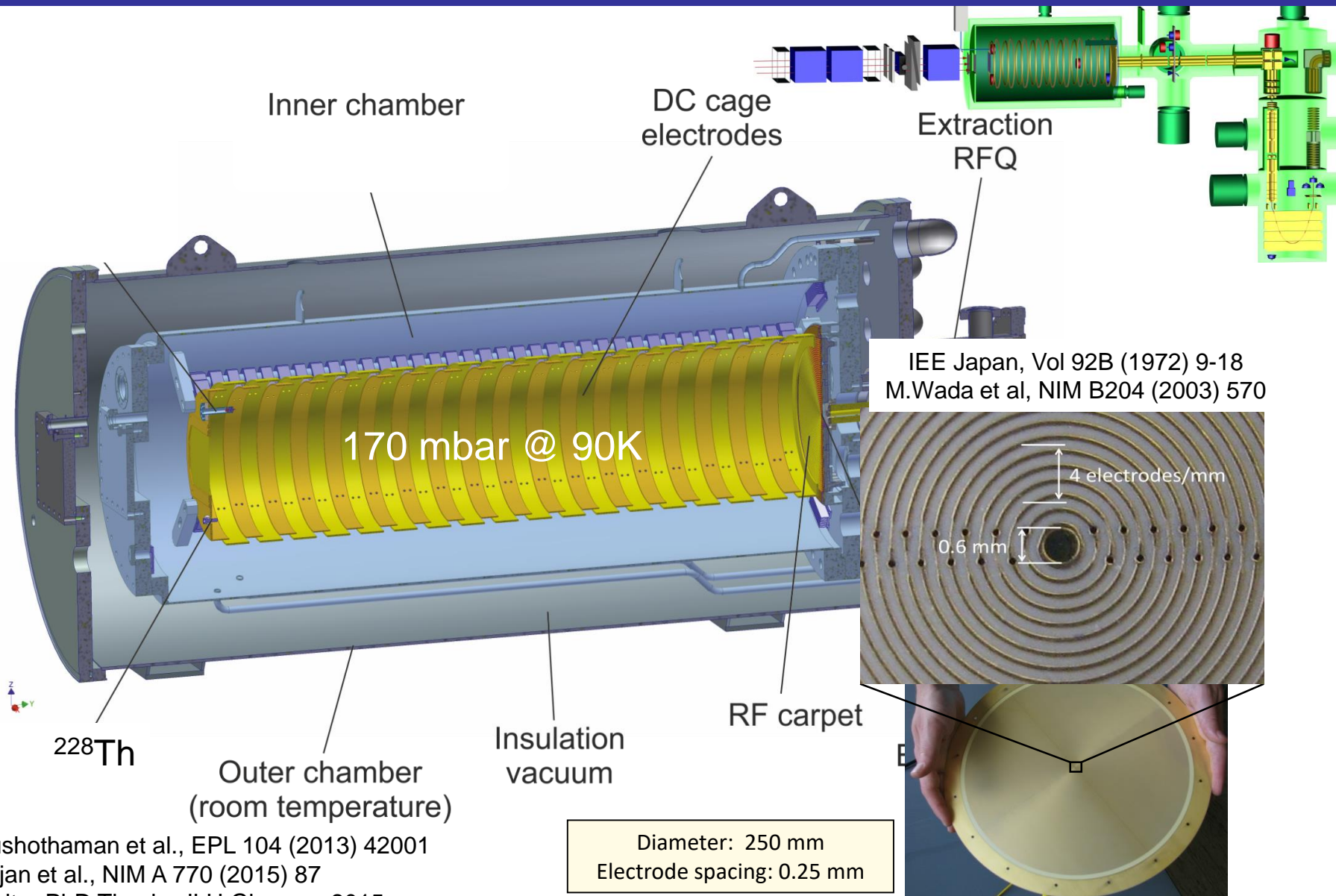
M. Wada NIM B 317 (2013) 450

Cryogenic Operation

- **Clean** \rightarrow ion beams of high cleanliness

M. Ranjan et al., Europhys. Lett. 96 (2011) 52001
Purushothaman S. et al, EPL 104 (2013) 42001

The cryogenic stopping cell at the FRS → ultrapure environment



IEE Japan, Vol 92B (1972) 9-18
 M.Wada et al, NIM B204 (2003) 570

^{228}Th

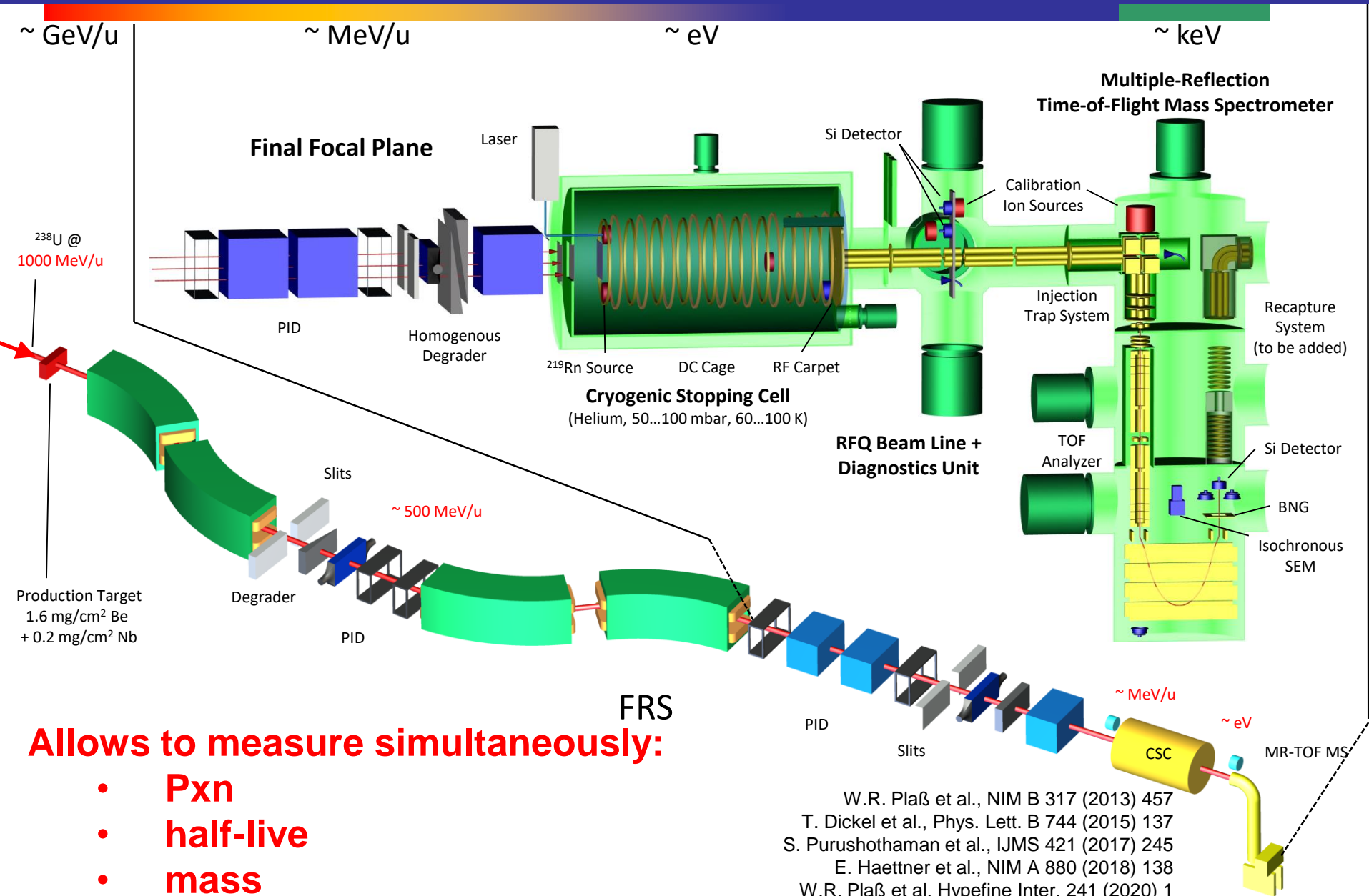
170 mbar @ 90K

4 electrodes/mm
 0.6 mm

Diameter: 250 mm
 Electrode spacing: 0.25 mm

- S. Purushothaman et al., EPL 104 (2013) 42001
- M. Ranjan et al., NIM A 770 (2015) 87
- M.P. Reiter PhD Thesis, JLU Giessen, 2015
- M.P. Reiter et al., NIM B 376 (2016) 240
- A.K. Rink PhD Thesis, JLU Giessen, 2017

FRS Ion Catcher



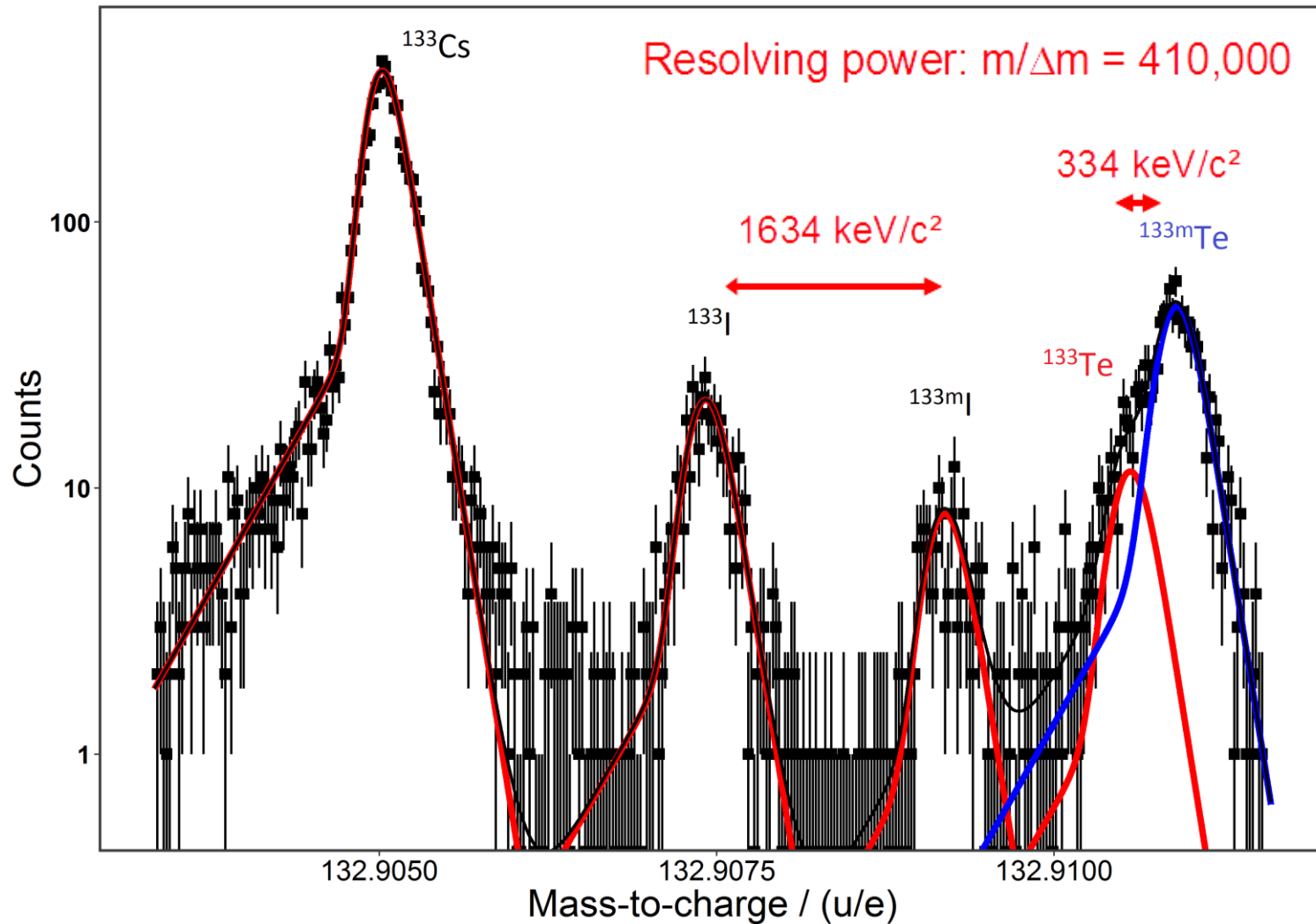
Allows to measure simultaneously:

- **Pxn**
- **half-live**
- **mass**

W.R. Plaß et al., NIM B 317 (2013) 457
 T. Dickel et al., Phys. Lett. B 744 (2015) 137
 S. Purushothaman et al., IJMS 421 (2017) 245
 E. Haettner et al., NIM A 880 (2018) 138
 W.R. Plaß et al, Hypefine Inter. 241 (2020) 1
 C. Hornung et al., PLB 802 (2020) 135200

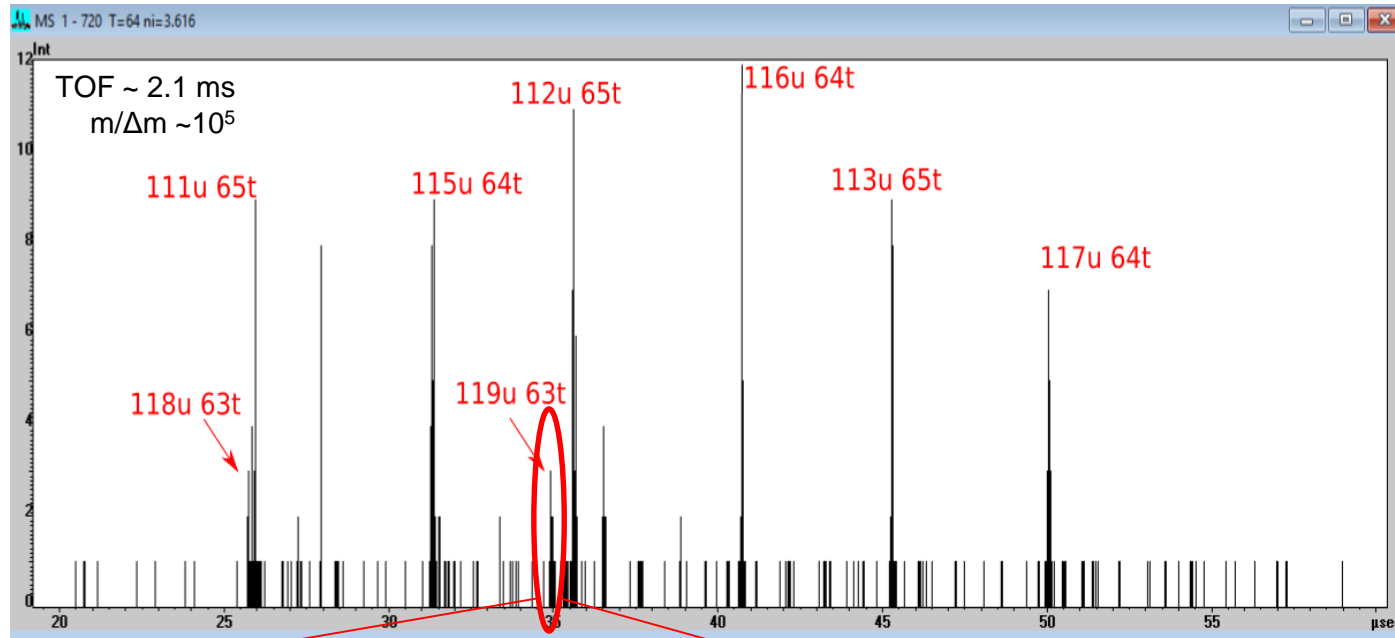
Mass measurements of Fission Fragments (In-Flight)

- Mass measurement of uranium fission products produced at 1000 MeV/u
- MR-TOF-MS will enable efficient search and measurement of new isotopes and isomers

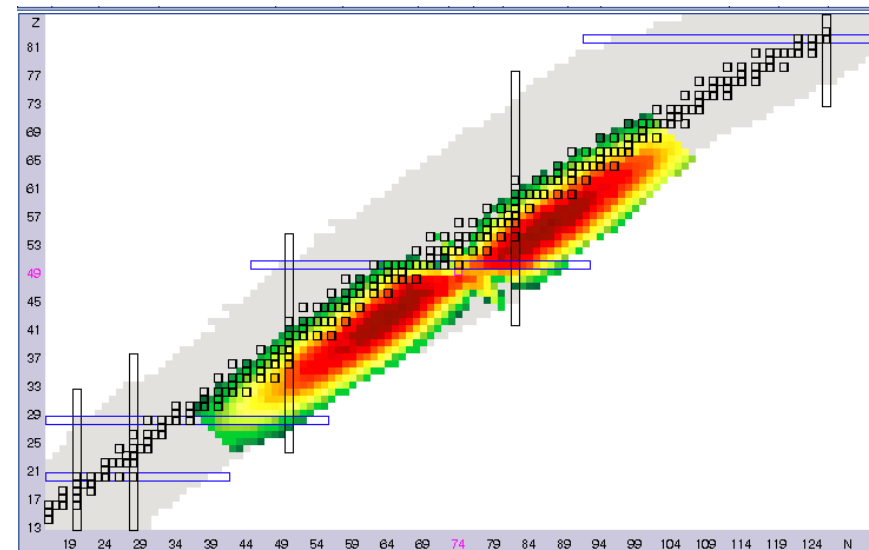
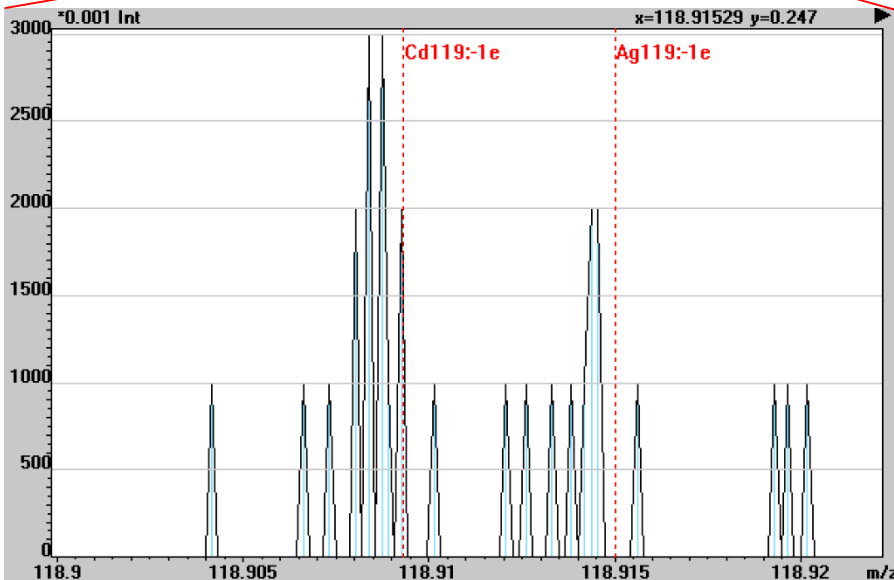


S. Ayet et al PRC 99, 064313 (2019)

Mass measurements of FF (spont. fission / in CSC)

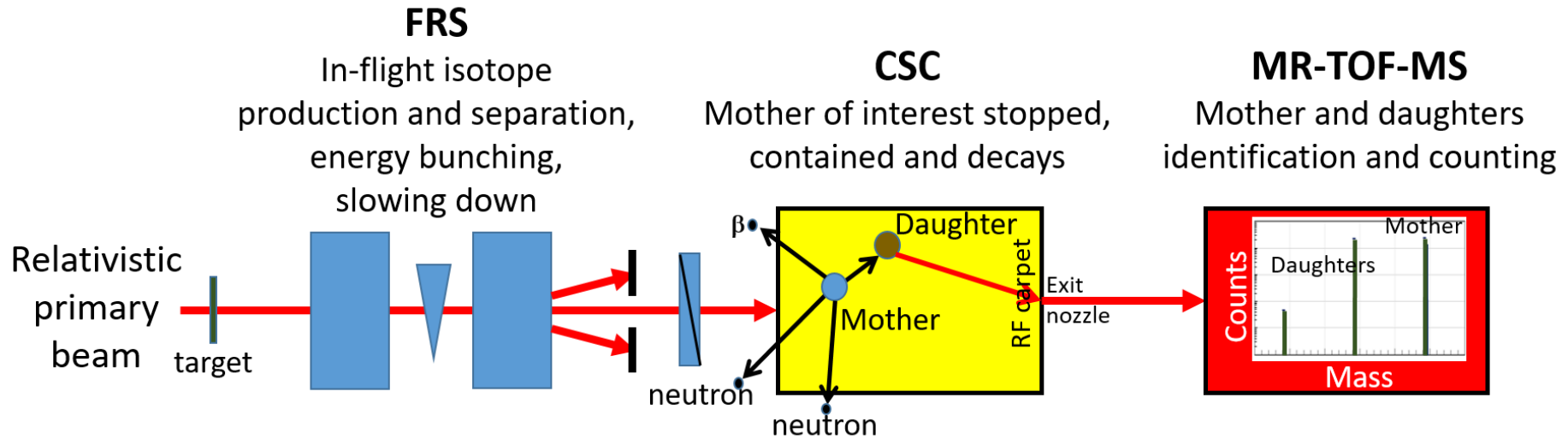


More than 15 fission fragments identified in a single one hour measurement, with a weak (37kBq) **252Cf** source

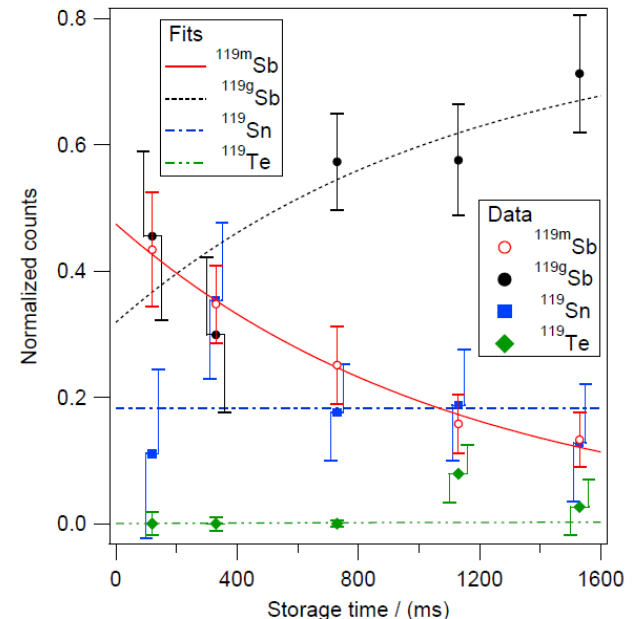


I. Mardor et al., EPJ Web of Conferences **239**, 02004 (2020)

PxN and half-life measurement with the FRS-IC



- P_{xn} is determined by the ratios between the daughters
- Method is **direct, essentially background free, with minimal systematic uncertainties, model independent and complementary** to worldwide programs
- Especially suited for **multi-neutron** emission probabilities



I. Miskun et al., Eur. Phys. J. A (2019) 55: 148

ELISOL RIB Facility

- Production of exotic neutron-rich fission fragments
- Focus on refractory elements: light region Zr-Mo-Rh and heavy rare-earths region around Ce

ELISOL beam line:

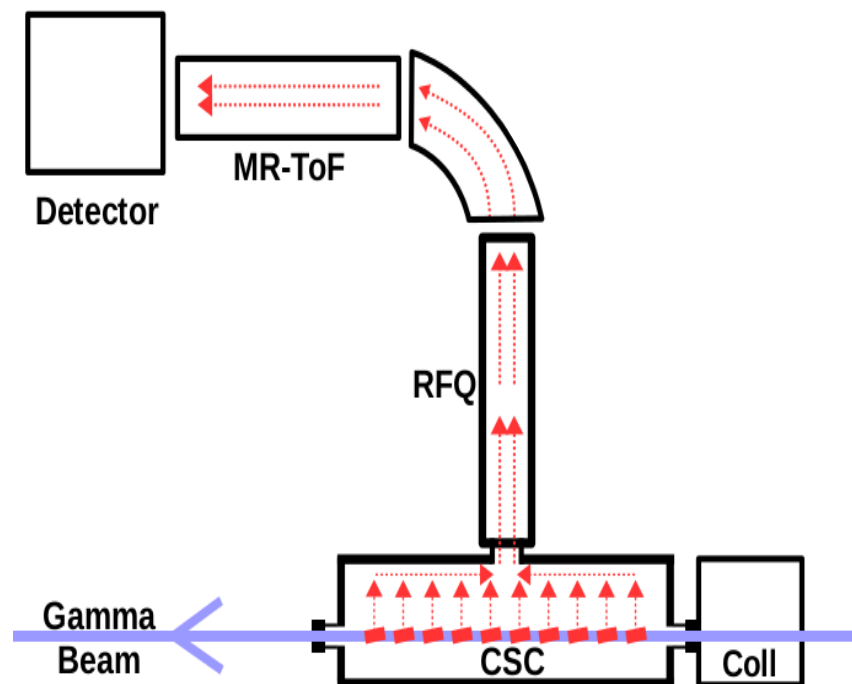
ELI-NP, GSI, Giessen, IFIN-HH, IPN Orsay, IoP VAST

Phase I

- 1) HADO-CSC (orthogonal extraction)
- 2) RFQ (Radio Frequency Quadrupole)
- 3) MR ToF (Multiple Reflection Time of Flight)

Phase II

- 1) β -decay station: HPGe detectors, tape station
- 2) collinear laser spectroscopy station



Conclusions

Fission plays an important role in the r-process

1. In the process itself: Fission re-cycling

nuclear physics to be studied:

Fission barrier and isotopic yields

2. Major production method to produce isotopes important for the understanding of the r-process

nuclear physics to be studied:

Ground state properties,

e.g. mass, half-live, P_{α} ,...

ELI-NP with its high brilliant and intense gamma beams and the suite of state-of-the-art detection will be at the forefront of this research

Acknowledgements

Thank you for your **attention** and

- A. Andreyev
 - D. Balabansky
 - O. Hall
 - I. Mardor
 - C. Scheidenberger
- for providing slides and material.

Questions?